Flussi dissipativi in tre dimensioni

Cluster di condizioni iniziali

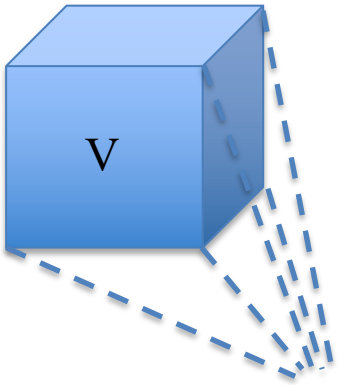

$$\frac{1}{V}\frac{dV}{dt} = \sum_{i=1}^{N}\frac{\partial f_i}{\partial x_i} \equiv div(f) \quad < 0$$

$$\begin{aligned} \dot{x}_1 &= f_1(x_1, x_2, x_3) \\ \dot{x}_2 &= f_2(x_1, x_2, x_3) \\ \dot{x}_3 &= f_3(x_1, x_2, x_3) \end{aligned}$$

ATTRATTORI

- fixed points (dim.0)
- limit cycles (dim.1)
- quasiperiodic attractors (dim.2)
- chaotic attractors (fractal dimension between 2 and 3)

Flussi dissipativi in tre dimensioni

Cluster di condizioni iniziali

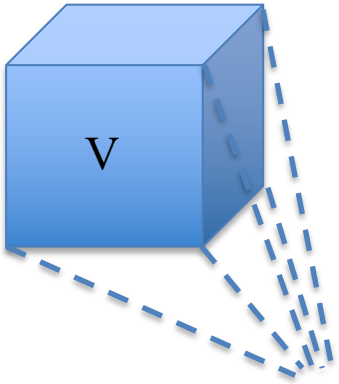

$$\frac{1}{V}\frac{dV}{dt} = \sum_{i=1}^{N} \frac{\partial f_i}{\partial x_i} \equiv div(f) \quad < 0$$

ATTRATTORI

fixed points (dim.0)

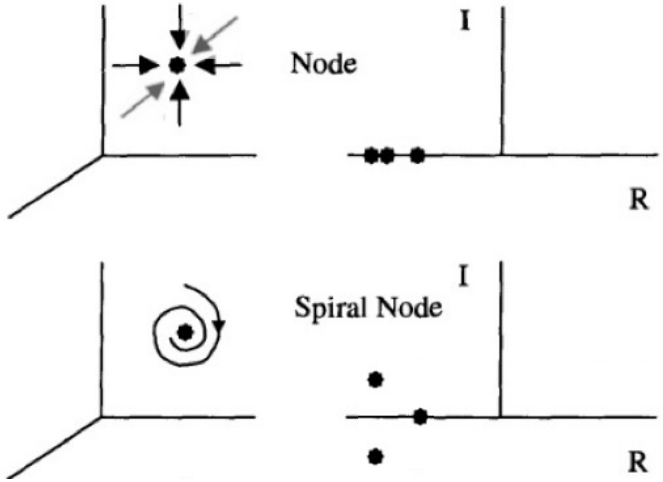

$$J = \begin{pmatrix} \frac{\partial f_1}{\partial x_1} & \frac{\partial f_1}{\partial x_2} & \frac{\partial f_1}{\partial x_3} \\ \frac{\partial f_2}{\partial x_1} & \frac{\partial f_2}{\partial x_2} & \frac{\partial f_2}{\partial x_3} \\ \frac{\partial f_3}{\partial x_1} & \frac{\partial f_3}{\partial x_2} & \frac{\partial f_3}{\partial x_3} \end{pmatrix}$$

Flussi dissipativi in tre dimensioni

Cluster di condizioni iniziali

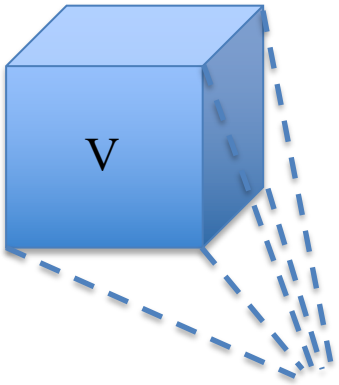

$$\frac{1}{V}\frac{dV}{dt} = \sum_{i=1}^{N} \frac{\partial f_i}{\partial x_i} \equiv div(f) \quad < 0$$

ATTRATTORI

fixed points (dim.0)

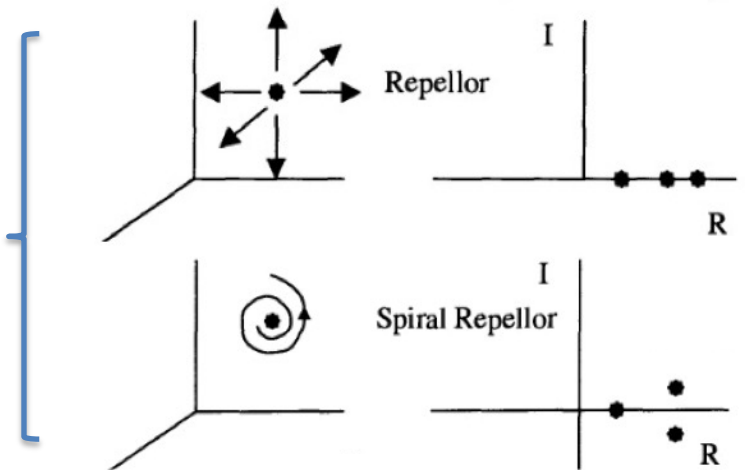

$$J = \begin{pmatrix} \frac{\partial f_1}{\partial x_1} & \frac{\partial f_1}{\partial x_2} & \frac{\partial f_1}{\partial x_3} \\ \frac{\partial f_2}{\partial x_1} & \frac{\partial f_2}{\partial x_2} & \frac{\partial f_2}{\partial x_3} \\ \frac{\partial f_3}{\partial x_1} & \frac{\partial f_3}{\partial x_2} & \frac{\partial f_3}{\partial x_3} \end{pmatrix}$$

Flussi dissipativi in tre dimensioni

Cluster di condizioni iniziali

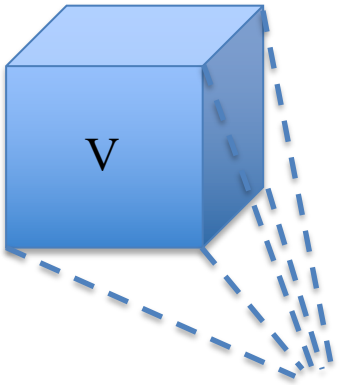

$$\frac{1}{V}\frac{dV}{dt} = \sum_{i=1}^{N} \frac{\partial f_i}{\partial x_i} \equiv div(f) \quad < 0$$

ATTRACTORI

fixed points (dim.0)

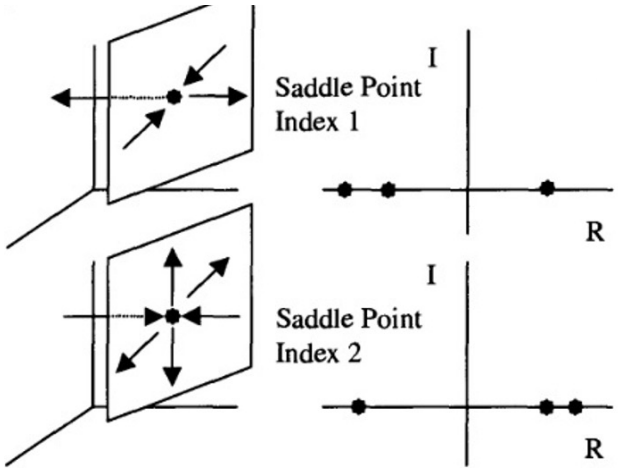

$$J = \begin{pmatrix} \frac{\partial f_1}{\partial x_1} & \frac{\partial f_1}{\partial x_2} & \frac{\partial f_1}{\partial x_3} \\ \frac{\partial f_2}{\partial x_1} & \frac{\partial f_2}{\partial x_2} & \frac{\partial f_2}{\partial x_3} \\ \frac{\partial f_3}{\partial x_1} & \frac{\partial f_3}{\partial x_2} & \frac{\partial f_3}{\partial x_3} \end{pmatrix}$$

Flussi dissipativi in tre dimensioni

Cluster di condizioni iniziali

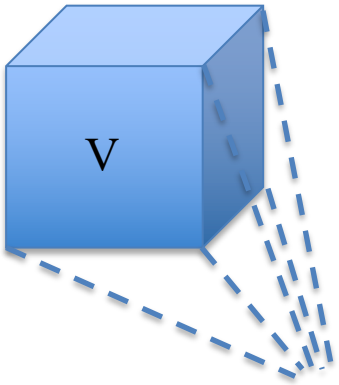

$$\frac{1}{V}\frac{dV}{dt} = \sum_{i=1}^{N} \frac{\partial f_i}{\partial x_i} \equiv div(f) \quad < 0$$

ATTRATTORI

fixed points (dim.0)

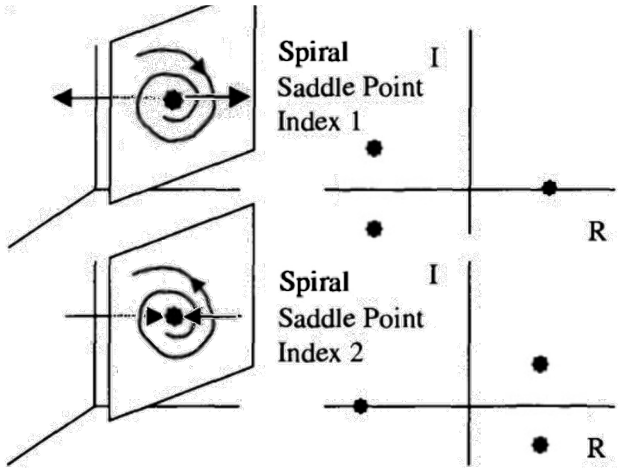

$$J = \begin{pmatrix} \frac{\partial f_1}{\partial x_1} & \frac{\partial f_1}{\partial x_2} & \frac{\partial f_1}{\partial x_3} \\ \frac{\partial f_2}{\partial x_1} & \frac{\partial f_2}{\partial x_2} & \frac{\partial f_2}{\partial x_3} \\ \frac{\partial f_3}{\partial x_1} & \frac{\partial f_3}{\partial x_2} & \frac{\partial f_3}{\partial x_3} \end{pmatrix}$$

Flussi dissipativi in tre dimensioni

Cluster di condizioni iniziali

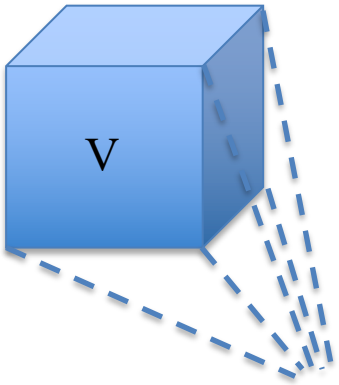

$$\frac{1}{V}\frac{dV}{dt} = \sum_{i=1}^{N}\frac{\partial f_i}{\partial x_i} \equiv div(f) \quad < 0$$

ATTRATTORI

limit cycles (dim.1)

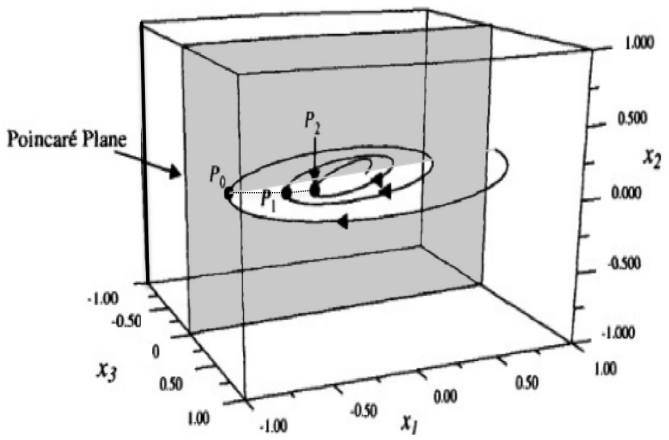

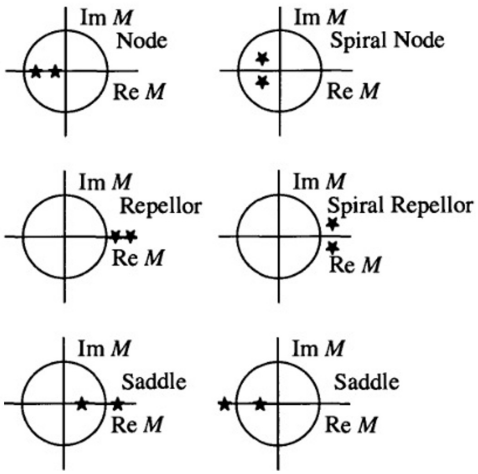

Flussi dissipativi in tre dimensioni

Cluster di condizioni iniziali

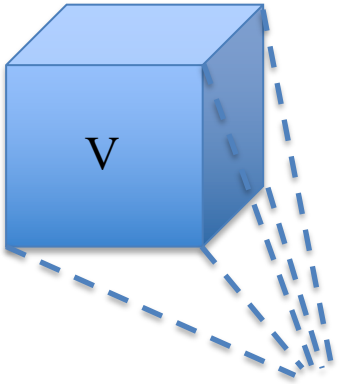

$$\frac{1}{V}\frac{dV}{dt} = \sum_{i=1}^{N} \frac{\partial f_i}{\partial x_i} \equiv div(f) \quad < 0$$

ATTRATTORI

limit cycles (dim.1)

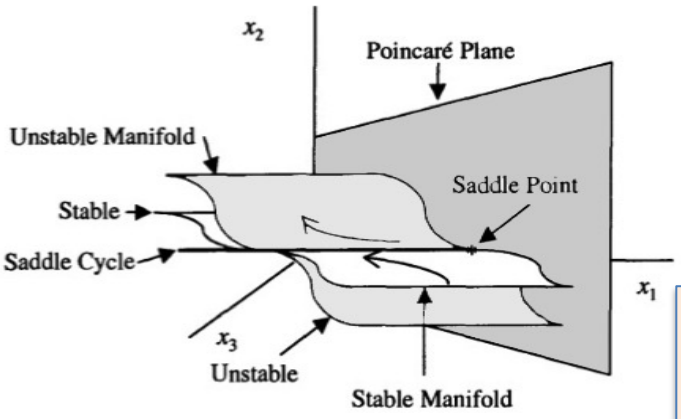

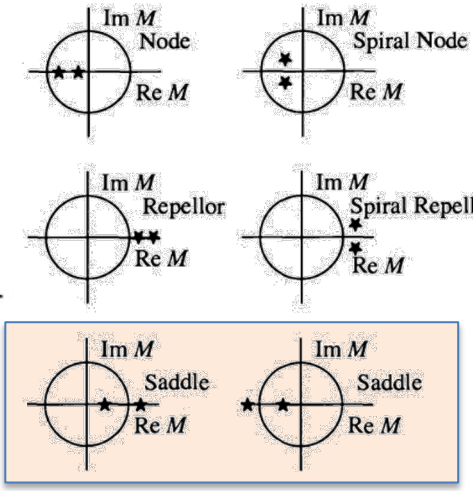

Flussi dissipativi in tre dimensioni

Cluster di condizioni iniziali

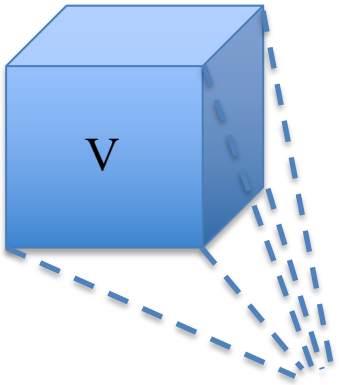

$$\frac{1}{V}\frac{dV}{dt} = \sum_{i=1}^{N}\frac{\partial f_i}{\partial x_i} \equiv div(f) \quad < 0$$

ATTRATTORI

quasiperiodic attractors (dim.2)

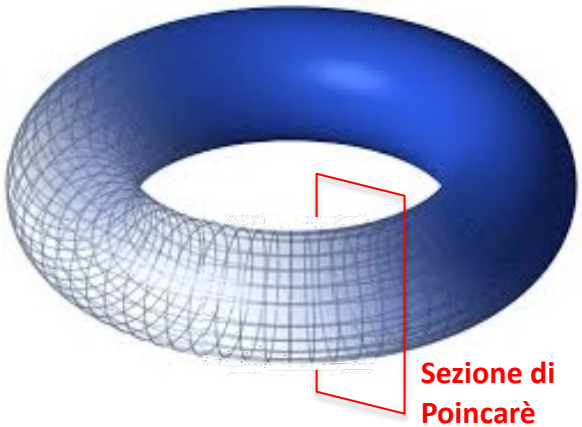

$\frac{\omega_R}{\omega_r}$ razionale

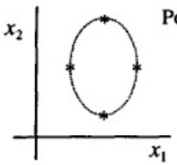

$\frac{\omega_R}{\omega_r}$ irrazionale

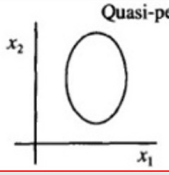

Flussi dissipativi in tre dimensioni

Cluster di condizioni iniziali

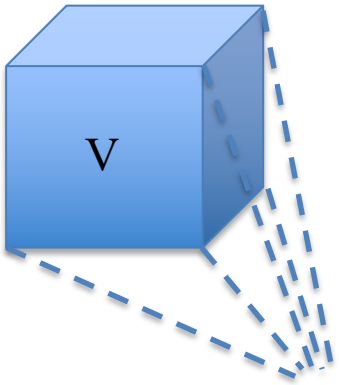

$$\frac{1}{V}\frac{dV}{dt} = \sum_{i=1}^{N}\frac{\partial f_i}{\partial x_i} \equiv div(f) \quad < 0$$

$$\begin{aligned} \dot{x}_1 &= f_1(x_1, x_2, x_3) \\ \dot{x}_2 &= f_2(x_1, x_2, x_3) \\ \dot{x}_3 &= f_3(x_1, x_2, x_3) \end{aligned}$$

ATTRATTORI

- fixed points (dim.0)
- limit cycles (dim.1)
- quasiperiodic attractors (dim.2)
- chaotic attractors (fractal dimension between 2 and 3)

Flussi dissipativi in tre dimensioni

Cluster di condizioni iniziali

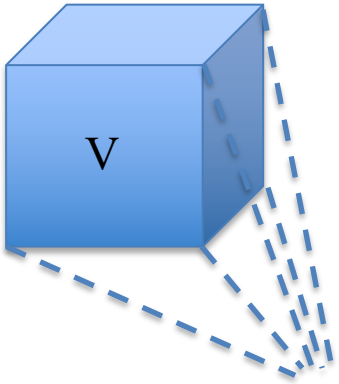

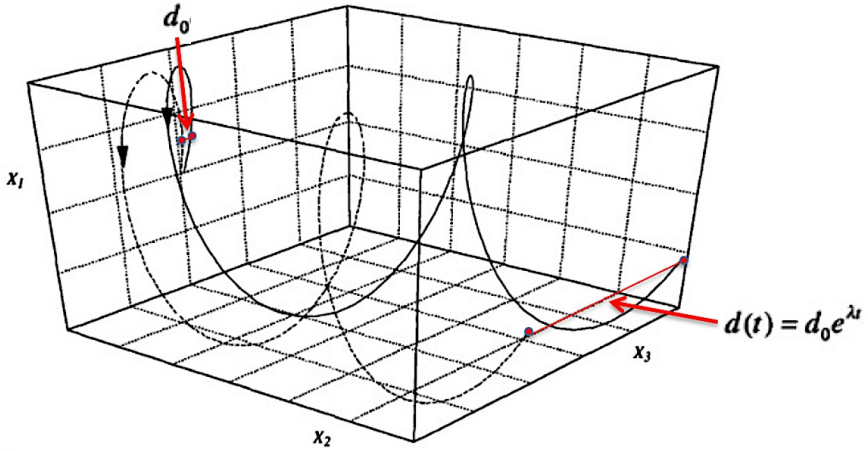

ATTRATTORI

1. no intersection of different trajectories;
2. bounded trajectories;
3. exponential divergence of nearby trajectories.

chaotic attractors (fractal dimension between 2 and 3)

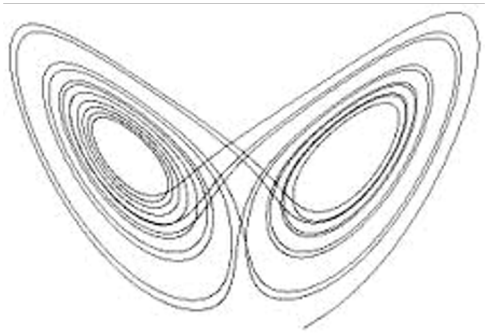

Rotte verso il CAOS...

I : Period-Doubling

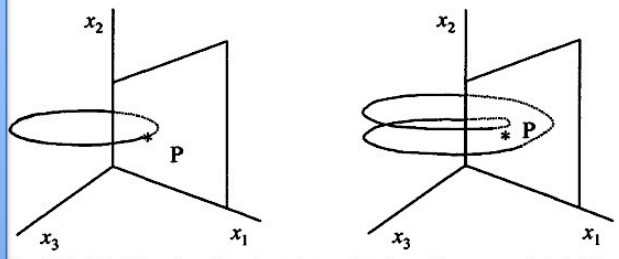

II : Quasi-Periodicity

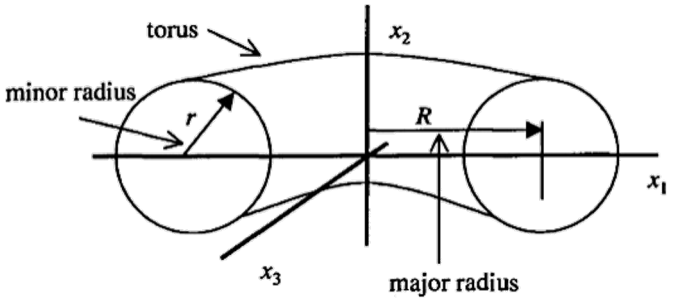

III : Intermittency and Crises

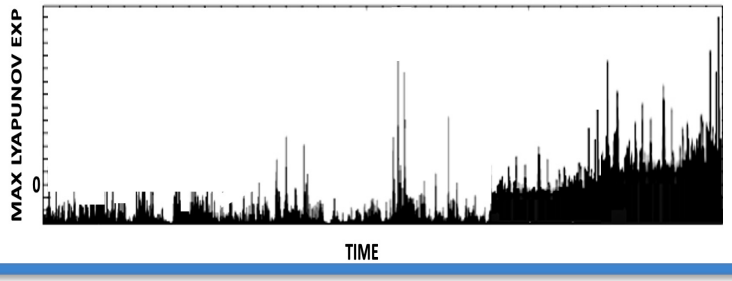

Local Bifurcations

Global Bifurcations

IV : Chaotic Transient and Homoclinic Orbits

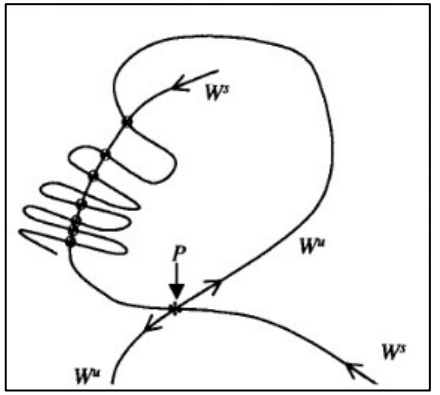

IV 4.11 The Routes to Chaos IV: Chaotic Transients and Homoclinic Orbits

3 dim: saddle cycle

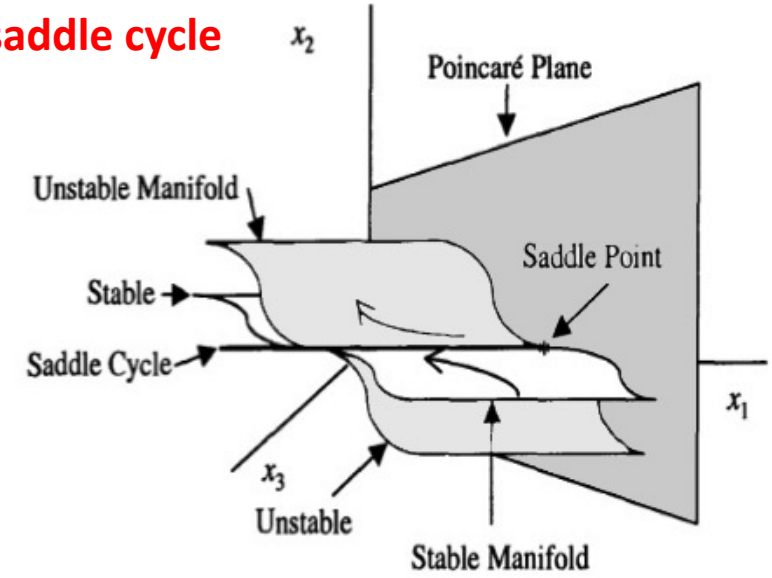

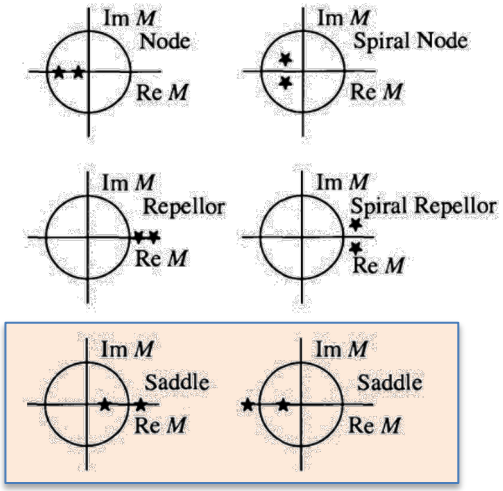

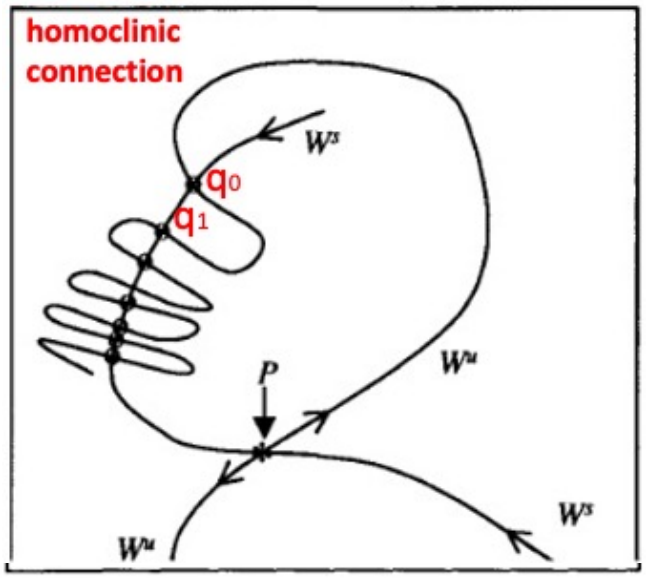

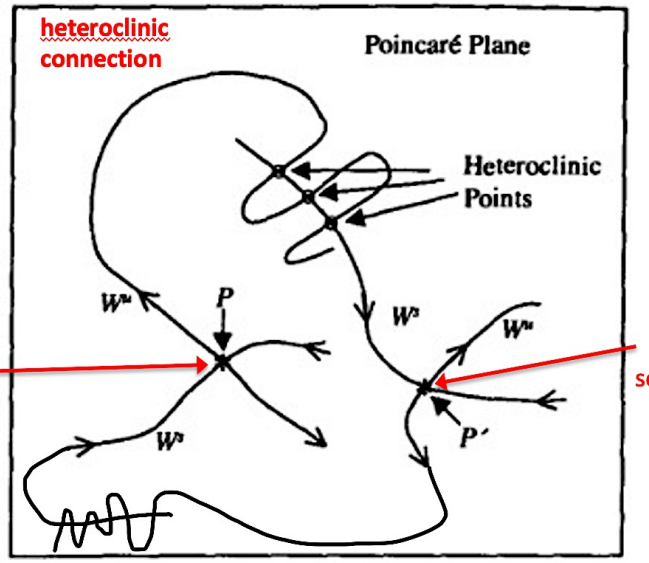

Saddle point P corrispondente al primo saddle cycle

Saddle point P' corrispondente al secondo saddle cycle

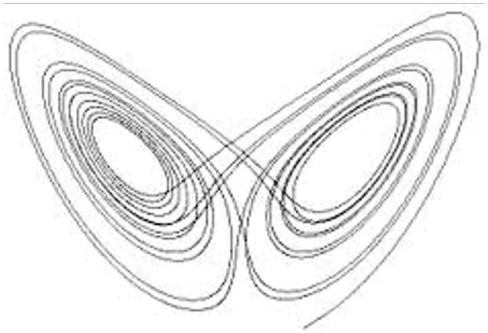

Rotte verso il CAOS...

IL MODELLO DI LORENZ

The Lorenz Equations

The Lorenz model is based on a (gross) simplification of the fundamental Navier–Stokes equations for fluids. As shown in Appendix C, the fluid motion and resulting temperature differences can be expressed in terms of three variables, conventionally called $X(t)$, $Y(t)$, and $Z(t)$.

$$\begin{cases} \dot{X} = p(Y - X) \\ \dot{Y} = -XZ + rX - Y \\ \dot{Z} = XY - bZ \end{cases}$$

Riproducono la dinamica delle Celle Convettive di Rayleigh-Bénard

generate dalla differenza di temperatura tra la superficie inferiore e quella superiore del recipiente contenente il fluido

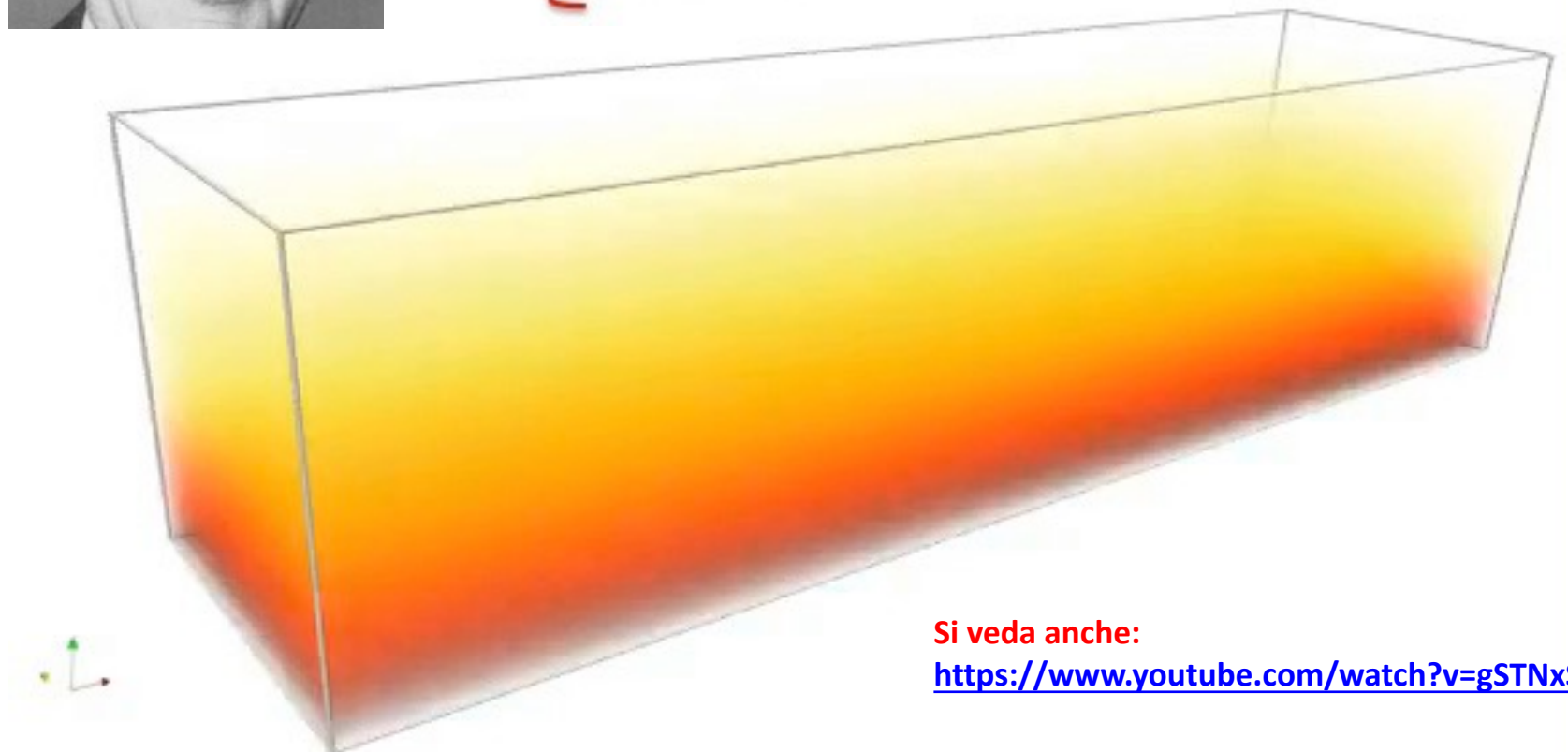

Si veda anche:
https://www.youtube.com/watch?v=gSTNxS96fRg

The Lorenz Equations

The Lorenz model is based on a (gross) simplification of the fundamental Navier–Stokes equations for fluids. As shown in Appendix C, the fluid motion and resulting temperature differences can be expressed in terms of three variables, conventionally called $X(t)$, $Y(t)$, and $Z(t)$.

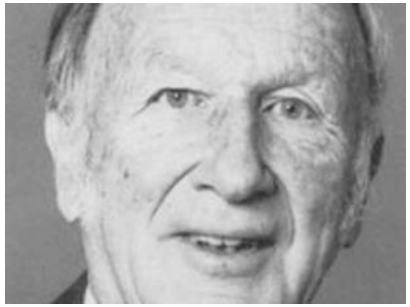

$$\begin{cases} \dot{X} = p(Y - X) \\ \dot{Y} = -XZ + rX - Y \\ \dot{Z} = XY - bZ \end{cases}$$

Significato delle 3 variabili:

X(t): dipendenza temporale della funzione di flusso del fluido (le cui derivate rispetto alle variabili spaziali rappresentano le componenti della velocità del fluido)

Y(t): dipendenza temporale della differenza di temperatura tra la parte ascendente e quella discendente del fluido

Z(t): dipendenza temporale della deviazione dalla linearità della temperatura in funzione della posizione verticale

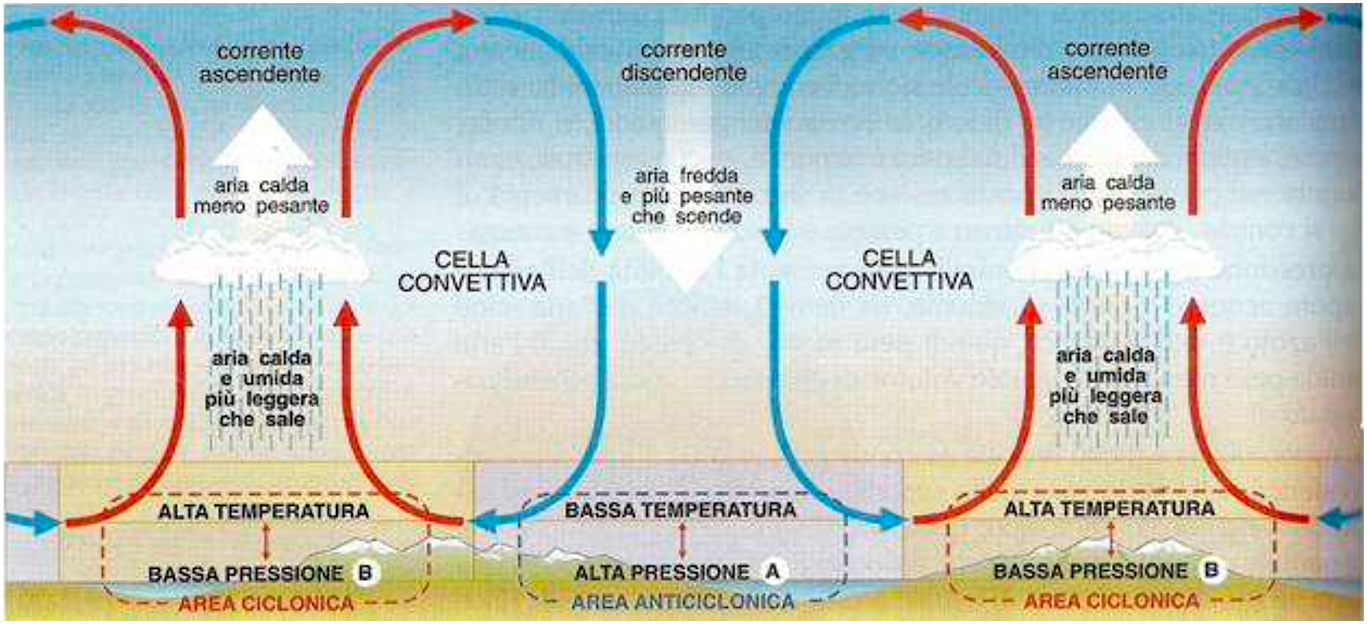

The Lorenz Equations

The Lorenz model is based on a (gross) simplification of the fundamental Navier–Stokes equations for fluids. As shown in Appendix C, the fluid motion and resulting temperature differences can be expressed in terms of three variables, conventionally called $X(t)$, $Y(t)$, and $Z(t)$.

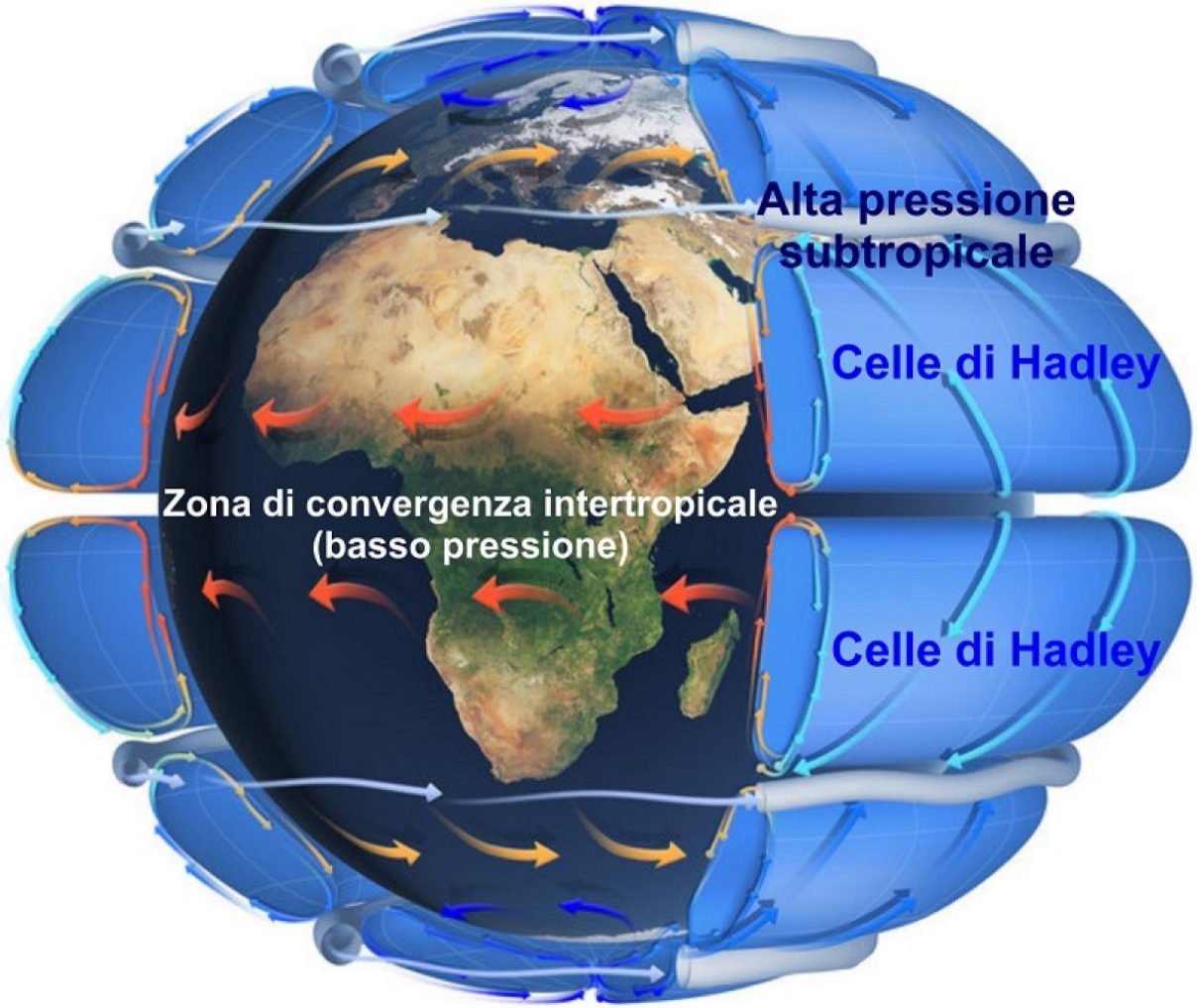

Significato delle 3 variabili:

X(t): dipendenza temporale della funzione di flusso del fluido (le cui derivate rispetto alle variabili spaziali rappresentano le componenti della velocità del fluido)

Y(t): dipendenza temporale della differenza di temperatura tra la parte ascendente e quella discendente del fluido

Z(t): dipendenza temporale della deviazione dalla linearità della temperatura in funzione della posizione verticale

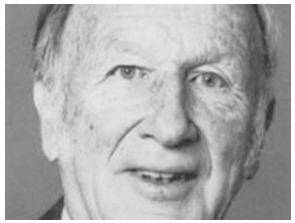

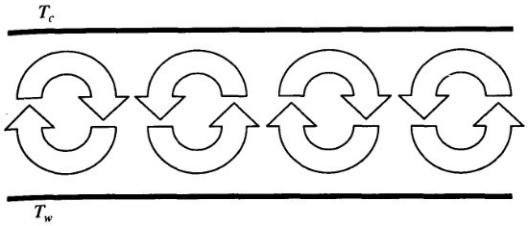

$$\begin{cases} \dot{X} = p(Y - X) \\ \dot{Y} = -XZ + rX - Y \\ \dot{Z} = XY - bZ \end{cases}$$

Significato dei 3 parametri di controllo:

Prandtl number p:
rapporto tra la viscosità cinetica del fluido e il coefficiente di diffusione termica

Rayleigh number r:
misura della differenza di temperatura tra la parte superiore e quella inferiore del fluido

Parameter b:
esprime il rapporto tra l'altezza verticale dello strato di fluido e la dimenzione orizzontale delle celle convettive

p, r, and b are adjustable parameters; p is the so-called Prandtl number, which is defined to be the ratio of the kinetic viscosity of the fluid to its thermal diffusion coefficient. In rough terms, the Prandtl number compares the rate of energy loss from a small "packet" of fluid due to viscosity (friction) to the rate of energy loss from the packet due to thermal conduction. r is proportional to the ***Rayleigh number***, which is a dimensionless measure of the temperature difference between the bottom and top of the fluid layer. As the temperature difference increases, the Rayleigh number increases. The final parameter b is related to the ratio of the vertical height h of the fluid layer to the horizontal size of the convection rolls. It turns out that for $b = 8/3$, the convection begins for the smallest value of the Rayleigh number, that is, for the smallest value of the temperature difference δT.

This is the value usually chosen for the study of the Lorenz model. p is then chosen for the particular fluid under study. Lorenz (LOR63) used the value $p = 10$ (which corresponds roughly to cold water), a value that had been used in a previous study of Rayleigh–Bénard convection by Saltzman (SAL62). We let r, the Rayleigh number, be the adjustable control parameter.

The Lorenz model, although based on what appears to be a very simple set of differential equations, exhibits very complex behavior. The equations look so simple that one is led to guess that it would be easy to write down their solutions, that is, to give X, Y, and Z as functions of time. In fact, as we shall discuss later, it is now believed that it is in principle impossible to give the solutions in analytic form, that is, to write down a formula that would give X, Y, and Z for any instant of time. Thus, we must solve the equations numerically, which, in practice, means that a computer does the numerical integration for us. Here, we will describe just a few results of such an integration. The analytic underpinnings for these results will be discussed later.

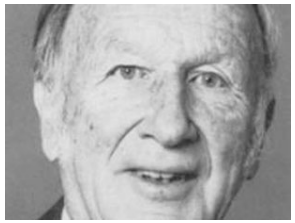

$$\begin{cases} \dot{X} = p(Y - X) \\ \dot{Y} = -XZ + rX - Y \\ \dot{Z} = XY - bZ \end{cases}$$

Significato dei 3 parametri di controllo:

Prandtl number p:
rapporto tra la viscosità cinetica del fluido e il coefficiente di diffusione termica **(p = 10)**

Rayleigh number r:
misura della differenza di temperatura tra la parte superiore e quella inferiore del fluido **(r = variabile)**

Parameter b:
esprime il rapporto tra l'altezza verticale dello strato di fluido e la dimenzione orizzontale delle celle convettive **(b = 8/3)**

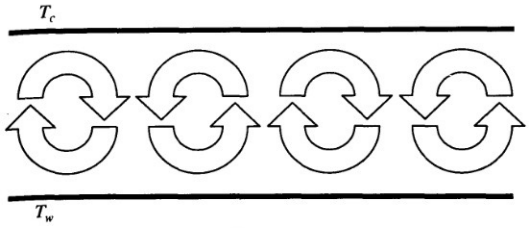

p, r, and b are adjustable parameters; p is the so-called Prandtl number, which is defined to be the ratio of the kinetic viscosity of the fluid to its thermal diffusion coefficient. In rough terms, the Prandtl number compares the rate of energy loss from a small "packet" of fluid due to viscosity (friction) to the rate of energy loss from the packet due to thermal conduction. r is proportional to the ***Rayleigh number***, which is a dimensionless measure of the temperature difference between the bottom and top of the fluid layer. As the temperature difference increases, the Rayleigh number increases. The final parameter b is related to the ratio of the vertical height h of the fluid layer to the horizontal size of the convection rolls. It turns out that for $b = 8/3$, the convection begins for the smallest value of the Rayleigh number, that is, for the smallest value of the temperature difference δT.

This is the value usually chosen for the study of the Lorenz model. p is then chosen for the particular fluid under study. Lorenz (LOR63) used the value $p = 10$ (which corresponds roughly to cold water), a value that had been used in a previous study of Rayleigh–Bénard convection by Saltzman (SAL62). We let r, the Rayleigh number, be the adjustable control parameter.

The Lorenz model, although based on what appears to be a very simple set of differential equations, exhibits very complex behavior. The equations look so simple that one is led to guess that it would be easy to write down their solutions, that is, to give X, Y, and Z as functions of time. In fact, as we shall discuss later, it is now believed that it is in principle impossible to give the solutions in analytic form, that is, to write down a formula that would give X, Y, and Z for any instant of time. Thus, we must solve the equations numerically, which, in practice, means that a computer does the numerical integration for us. Here, we will describe just a few results of such an integration. The analytic underpinnings for these results will be discussed later.

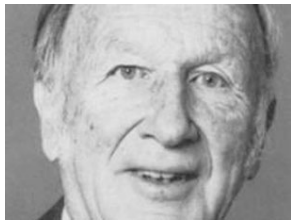

$$\dot{X} = p(Y - X)$$
$$\dot{Y} = -XZ + rX - Y$$
$$\dot{Z} = XY - bZ$$

p=10, b=8/3

STATO NON CONVETTIVO

r < 1

Behavior of Solutions to the Lorenz Equations

For small values of the parameter r, that is, for small temperature differences δT, the model predicts that the stationary, nonconvecting state is the stable condition. In terms of the variables X, Y, and Z, this state is described by the values $X = 0$, $Y = 0$, and $Z = 0$. For values of r just greater than 1, steady convection sets in. There are two possible convective states: one corresponding to clockwise rotation, the other to counterclockwise for a given convective roll. As we shall see, some initial conditions lead to one state, other conditions to the other state. Lord Rayleigh showed that if $p > b + 1$, then this steady convection is unstable for large enough r and gives way to more complex behavior. As r increases, the behavior has regions of chaotic behavior intermixed with regions of periodicity and regions of "intermittency," which cycle back and forth, apparently randomly, between chaotic and periodic behavior.

r < 1

r > 1

To illustrate some of this behavior, let us start our examination of the Lorenz model by looking at the behavior of the system for values of r less than 1. Rayleigh's analysis predicts that the system should settle into the steady, nonconvective state indicated by $X = 0$, $Y = 0$, $Z = 0$. Figure 1.17 shows the results of a numerical integration of the Lorenz equations starting from the initial state $X = 0$, $Y = 1$, $Z = 0$; that is, we have started the system with a small amount of circulation and slight temperature deviations. As time goes on, however, the system relaxes to the steady nonconvective state at $X = 0$, $Y = 0$, $Z = 0$.

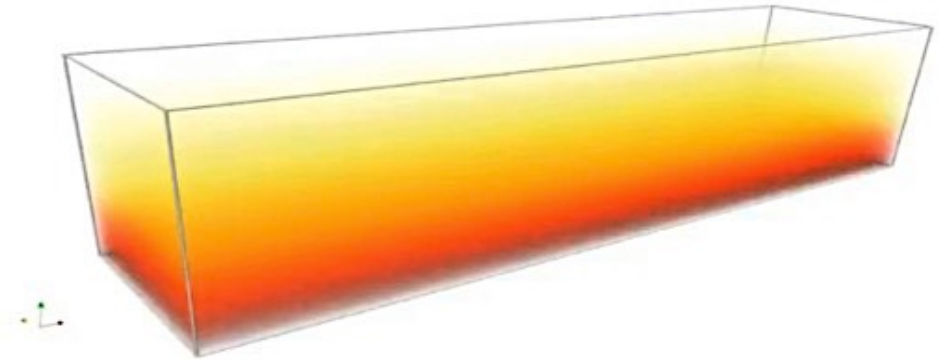

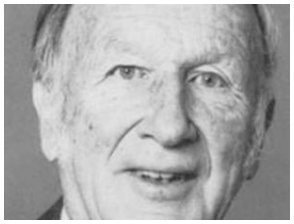

$$\dot{X} = p(Y - X)$$
$$\dot{Y} = -XZ + rX - Y$$
$$\dot{Z} = XY - bZ$$

p=10, b=8/3

Behavior of Solutions to the Lorenz Equations

For small values of the parameter r, that is, for small temperature differences δT, the model predicts that the stationary, nonconvecting state is the stable condition. In terms of the variables X, Y, and Z, this state is described by the values $X = 0$, $Y = 0$, and $Z = 0$. For values of r just greater than 1, steady convection sets in. There are two possible convective states: one corresponding to clockwise rotation, the other to counterclockwise for a given convective roll. As we shall see, some initial conditions lead to one state, other conditions to the other state. Lord Rayleigh showed that if $p > b + 1$, then this steady convection is unstable for large enough r and gives way to more complex behavior. As r increases, the behavior has regions of chaotic behavior intermixed with regions of periodicity and regions of "intermittency," which cycle back and forth, apparently randomly, between chaotic and periodic behavior.

r < 1

STATO NON CONVETTIVO

r < 1

X=0: la funzione di flusso del fluido è nulla

Y=0: non c'è differenza di temperatura tra la parte ascendente e quella discendente del fluido

Z=0: non c'è deviazione dalla linearità della temperatura in funzione della posizione verticale

WolframAlpha

{{10(y-x)},{-xz+rx-y},{xy-(8/3)z}}

Real root

$$x = 0, \quad y = 0, \quad z = 0$$

Roots

$$x = -2\sqrt{\frac{2}{3}}\sqrt{r-1}, \quad y = -2\sqrt{\frac{2}{3}}\sqrt{r-1}, \quad z = r-1$$

$$x = 2\sqrt{\frac{2}{3}}\sqrt{r-1}, \quad y = 2\sqrt{\frac{2}{3}}\sqrt{r-1}, \quad z = r-1$$

UNICO PUNTO FISSO REALE

SARA' STABILE?

4.5 Fixed Points in Three Dimensions (dim = 0)

The fixed points of the system of Eqs. (4.4-1) are found, of course, by setting the three time derivatives equal to 0. [Two-dimensional forced systems, even if written in the three-dimensional form (4.4-4), do not have any fixed points because, as the last of Eqs. (4.4-4) shows, we never have $\dot{x}_3 = t = 0$. Thus, we will need other techniques to deal with them.] The nature of each of the fixed points is determined by the three characteristic values of the Jacobian matrix of partial derivatives evaluated at the fixed point in question. The Jacobian matrix is

$$J = \begin{pmatrix} \frac{\partial f_1}{\partial x_1} & \frac{\partial f_1}{\partial x_2} & \frac{\partial f_1}{\partial x_3} \\ \frac{\partial f_2}{\partial x_1} & \frac{\partial f_2}{\partial x_2} & \frac{\partial f_2}{\partial x_3} \\ \frac{\partial f_3}{\partial x_1} & \frac{\partial f_3}{\partial x_2} & \frac{\partial f_3}{\partial x_3} \end{pmatrix} \qquad (4.5\text{-}1)$$

In finding the characteristic values of this matrix, we will generally have a cubic equation, whose roots will be the three characteristic values labeled $\lambda_1, \lambda_2, \lambda_3$.

4.5 Fixed Points in Three Dimensions (dim = 0)

The fixed points of the system of Eqs. (4.4-1) are found, of course, by setting the three time derivatives equal to 0. [Two-dimensional forced systems, even if written in the three-dimensional form (4.4-4), do not have any fixed points because, as the last of Eqs. (4.4-4) shows, we never have $\dot{x}_3 = t = 0$. Thus, we will need other techniques to deal with them.] The nature of each of the fixed points is determined by the three characteristic values of the Jacobian matrix of partial derivatives evaluated at the fixed point in question. The Jacobian matrix is

Jacobiano del modello di Lorenz, da calcolare in corrispondenza di ciascun punto fisso

$$J = \begin{pmatrix} -p & p & 0 \\ r - Z & -1 & -X \\ Y & X & -b \end{pmatrix} \qquad (4.5\text{-}1)$$

In finding the characteristic values of this matrix, we will generally have a cubic equation, whose roots will be the three characteristic values labeled $\lambda_1, \lambda_2, \lambda_3$.

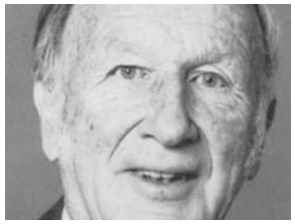

STUDIO DELLA STABILITA' DEL PUNTO FISSO:

X=0

Y=0

Z=0

(UNICO PUNTO FISSO PER 0<r<1)

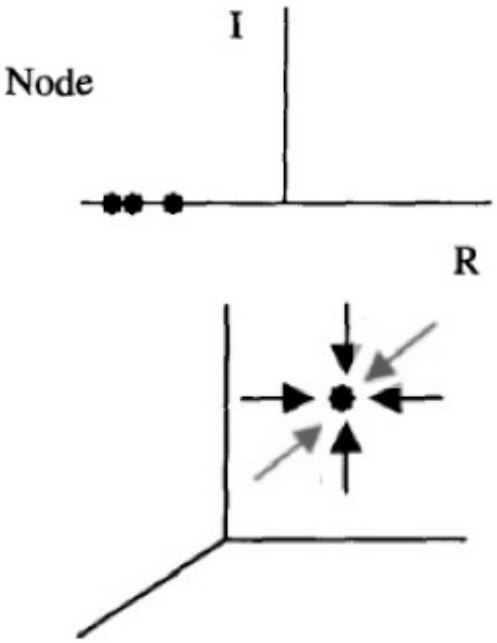

WolframAlpha computational... knowledge engine

{{-p,p,0},{(r-z),-1,-x},{y,x,-b}} where p=10,b=8/3,r=0.5,x=0,y=0,z=0

Examples Random

r = 0.5

Input interpretation:

$$\begin{pmatrix} -p & p & 0 \\ r-z & -1 & -x \\ y & x & -b \end{pmatrix} \text{ where } p = 10,\ b = \frac{8}{3},\ r = 0.5,\ x = 0,\ y = 0,\ z = 0$$

Result:

$$\left\{\{-10,\ 10,\ 0\},\ \{0.5,\ -1,\ 0\},\ \left\{0,\ 0,\ -\frac{8}{3}\right\}\right\}$$

Characteristic polynomial:

$$-x^3 - 13.6667\,x^2 - 34.3333\,x - 13.3333$$

Eigenvalues:

$$\lambda_1 \approx -10.5249$$

$$\lambda_2 \approx -2.66667$$

$$\lambda_3 \approx -0.475062$$

Eigenvectors:

$$v_1 \approx (-0.998625,\ 0.0524216,\ 0.)$$

$$v_2 \approx (0.,\ 0.,\ 1.)$$

$$v_3 \approx (-0.724097,\ -0.689698,\ 0.)$$

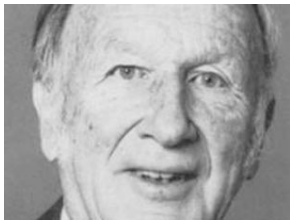

$$\dot{X} = p(Y - X)$$
$$\dot{Y} = -XZ + rX - Y$$
$$\dot{Z} = XY - bZ$$

p=10, b=8/3

r = 0.5

It will be useful to look at this behavior in two complementary graphic presentations. One graph plots the variables X, Y, and Z as functions of time, as in Fig. 1.17(a–c). The other graphs display the evolution of the system by following the motion of a point in XYZ space. Since the variables X, Y, and Z specify the state of the system for the Lorenz model, we call this space the ***state space*** for the system. For the Lorenz model, the state space is three-dimensional. We will usually follow the system with a two-dimensional projection, say on the XY or ZX planes of this state space. As time goes on, the point in state space will follow a path, which we shall call a trajectory. Figure 1.17(d) shows a ZX plane projection of the trajectory in state space. From Fig. 1.17, we see that the trajectory "relaxes" to the condition $X = 0$, $Y = 0$, and $Z = 0$ corresponding to the nonconvecting state illustrated in Fig. 1.15.

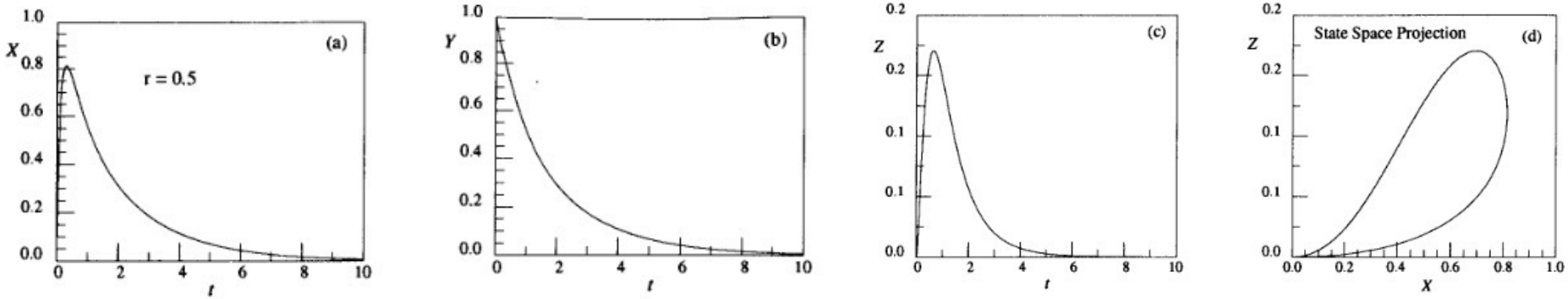

Fig. 1.17. In (a), (b), and (c), X, Y, and Z are plotted as functions of time for the Lorenz model with $r = 0.5$, $p = 10$, and $b = 8/3$. In (d), the trajectory is shown as a projection onto the ZX plane of state space. In all cases the trajectory started at the initial point $X = 0$, $Y = 1$, $Z = 0$.

lorenz-model.nlogo

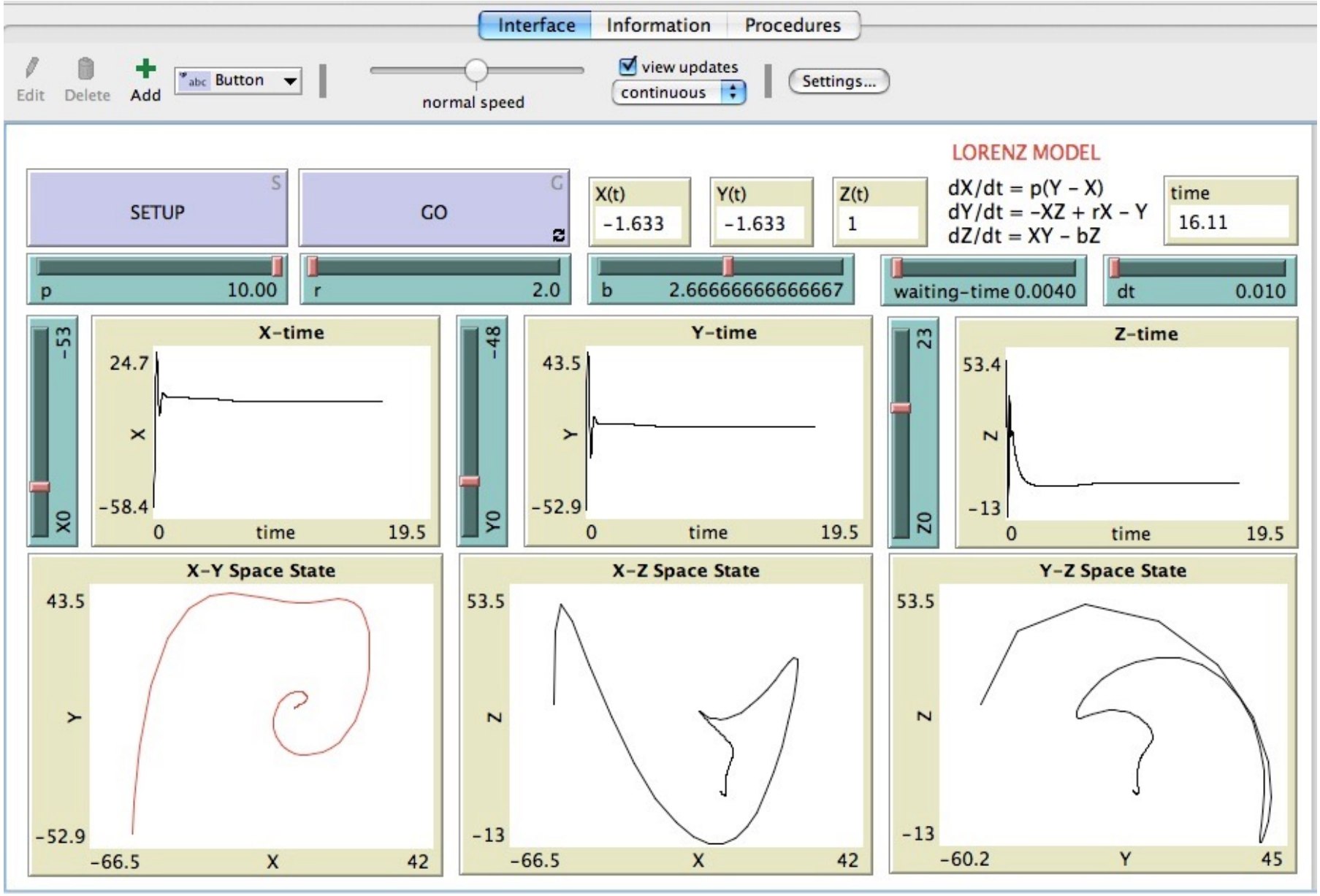

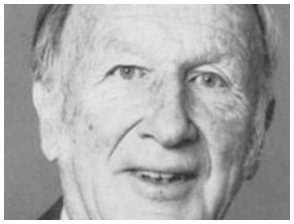

$$\begin{cases} \dot{X} = p(Y - X) \\ \dot{Y} = -XZ + rX - Y \\ \dot{Z} = XY - bZ \end{cases}$$

p=10, b=8/3

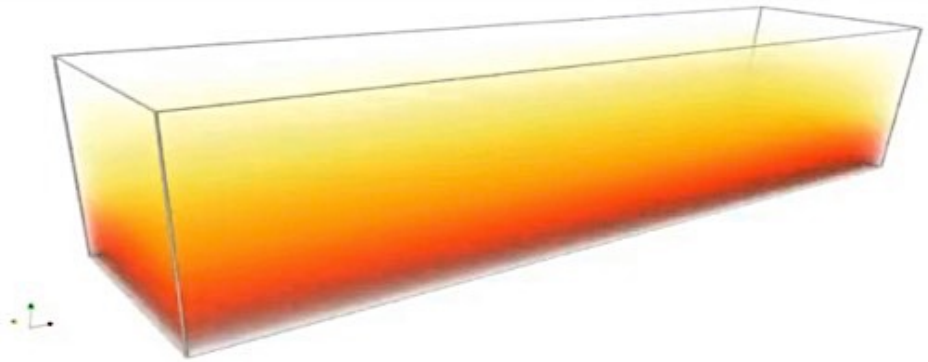

RIEPILOGO PARZIALE:

- **r < 1:** un unico **nodo** nell'origine.

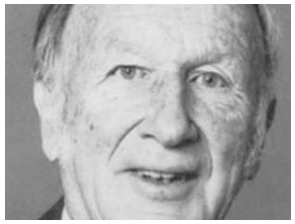

$$\dot{X} = p(Y - X)$$
$$\dot{Y} = -XZ + rX - Y$$
$$\dot{Z} = XY - bZ$$

p=10, b=8/3

For r values less than 1, all trajectories, no matter what their initial conditions, eventually end up approaching the fixed point at the origin of our XYZ state space. To use the language introduced for the logistic map, we can say that for $r < 1$, all of the XYZ space is the *basin of attraction* for the *attractor* at the origin.

For $r > 1$, we have three fixed points. The one at the origin turns out to be a repelling fixed point in the sense that trajectories starting near it tend to move away from it. The other two fixed points are attracting fixed points if r is not too large. Some initial conditions give rise to trajectories that approach one of the fixed points; other initial conditions give rise to trajectories that approach the other fixed point. (In Chapter 4, we will see more quantitatively what is different about these fixed points.) For r just greater than 1, the other two fixed points become the attractors in the state space. Thus, we say that $r = 1$ is a bifurcation point for the Lorenz model.

r > 1

NASCONO GLI ALTRI DUE PUNTI FISSI REALI FUORI DALL'ORIGINE, CHE CORRISPONDONO A STATI CONVETTIVI

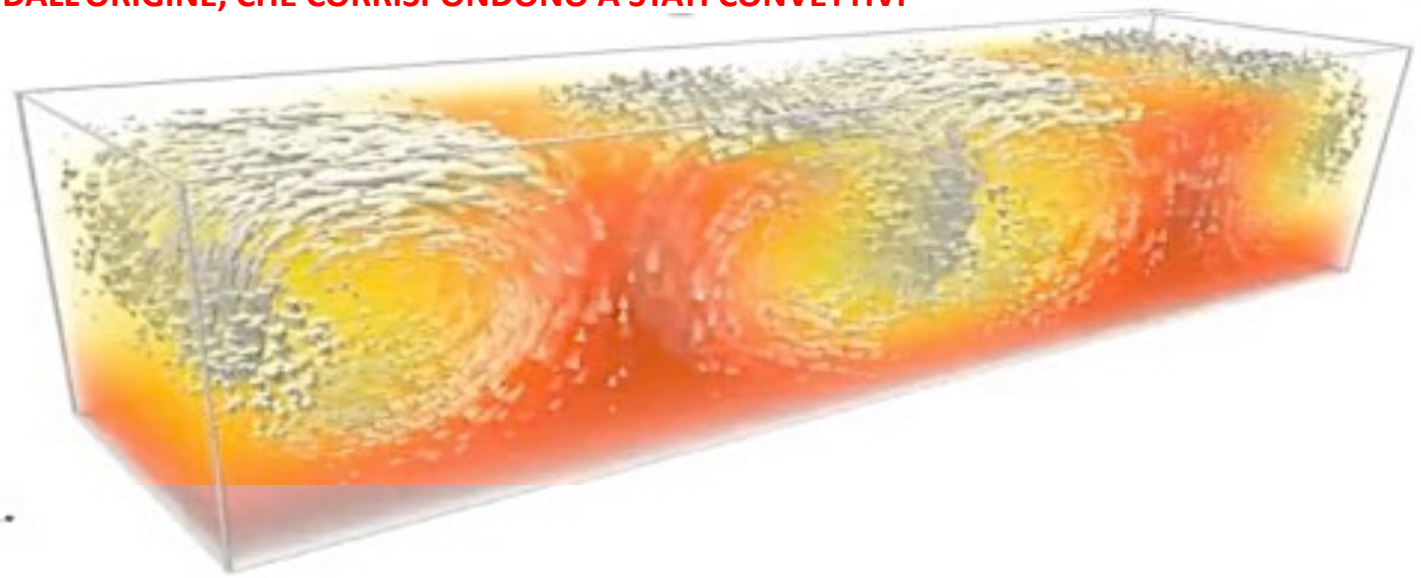

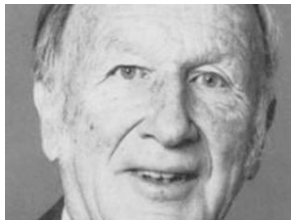

$$\begin{aligned}\dot{X} &= p(Y - X)\\ \dot{Y} &= -XZ + rX - Y\\ \dot{Z} &= XY - bZ\end{aligned}$$

p=10, b=8/3

r = 2

$$X = Y = \pm\sqrt{8/3} = \pm 1.63\ldots$$

Figure 1.18 illustrates the behavior of two trajectories starting from different initial points.

Let us describe this behavior in more physical terms. If r increases to a value just greater than 1 (recall that this means that we have increased the temperature difference between the bottom and top of the fluid layer), the fixed point at the origin becomes a repelling fixed point. This tells us that the so-called conductive state (the state with no fluid convection) has become unstable. The slightest deviation from the conditions $X = 0$, $Y = 0$, $Z = 0$ sends the state space trajectory away from the origin. For r just greater than 1, the trajectories are attracted to one or the other of the other two fixed points at $X = Y = \pm\sqrt{b(r-1)}$. Those two fixed points correspond to steady (time-independent) convection, one with clockwise rotation, the other counterclockwise. Some initial conditions give rise to trajectories that head toward one fixed point; other initial conditions lead to the other fixed point. The left-hand side of Fig. 1.18 shows the YZ plane state space projection for a trajectory starting from $X = 0$, $Y = -1$, $Z = 0$. The right-hand side of Fig. 1.18 shows a trajectory starting from a different set of initial values: $X = 0$, $Y = +1$, $Z = 0$. Note, in particular, that the system settles into a state with nonzero values of Y and Z, that is, the fluid is circulating.

WolframAlpha

{{10(y-x)},{-xz+2x-y},{xy-(8/3)z}}

Roots:

$x = 0, \quad y = 0, \quad z = 0$

$x = -2\sqrt{\frac{2}{3}}, \quad y = -2\sqrt{\frac{2}{3}}, \quad z = 1$

$x = 2\sqrt{\frac{2}{3}}, \quad y = 2\sqrt{\frac{2}{3}}, \quad z = 1$

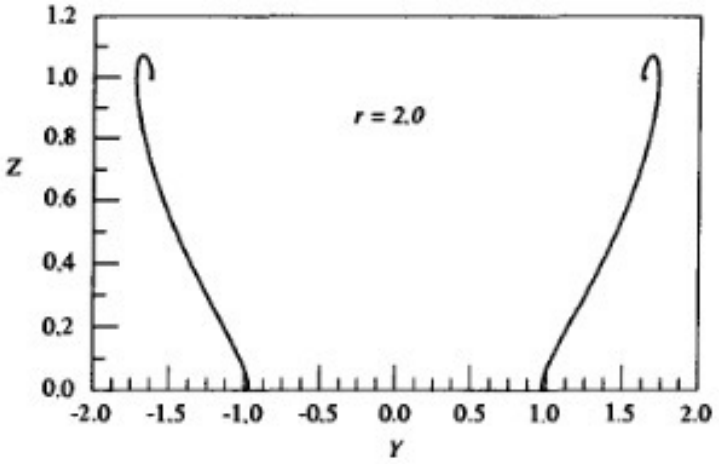

Fig. 1.18. State space projections onto the YZ plane for trajectories in the Lorenz model with $r = 2$. One attractor corresponds to clockwise rotation, the other to counterclockwise rotation of the fluid at a particular spatial location.

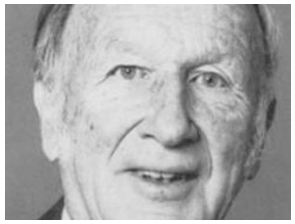

STUDIO DELLA STABILITA' DEL PUNTO FISSO:

X=0

Y=0

Z=0

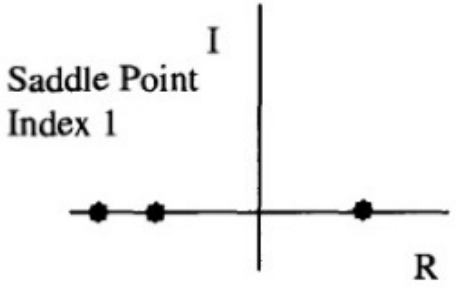

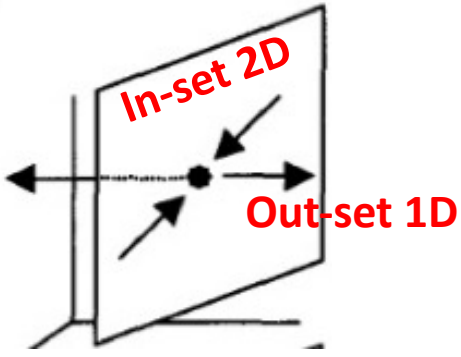

WolframAlpha computational... knowledge engine

{{-p,p,0},{(r-z),-1,-x},{y,x,-b}} where p=10,b=8/3,r=2,x=0,y=0,z=0

Examples Random

r = 2

Input interpretation:

$$\begin{pmatrix} -p & p & 0 \\ r-z & -1 & -x \\ y & x & -b \end{pmatrix} \text{ where } p = 10,\ b = \frac{8}{3},\ r = 2,\ x = 0,\ y = 0,\ z = 0$$

Result:

$$\left\{\{-10,\ 10,\ 0\},\ \{2,\ -1,\ 0\},\ \left\{0,\ 0,\ -\frac{8}{3}\right\}\right\}$$

Characteristic polynomial:

$$-x^3 - \frac{41\,x^2}{3} - \frac{58\,x}{3} + \frac{80}{3}$$

Eigenvalues: Exact forms

$\lambda_1 \approx -11.8443$

$\lambda_2 \approx -2.66667$

$\lambda_3 \approx 0.844289$

Eigenvectors: Exact forms

$v_1 \approx (-5.42214,\ 1.,\ 0.)$

$v_2 \approx (0.,\ 0.,\ 1.)$

$v_3 \approx (0.922144,\ 1.,\ 0.)$

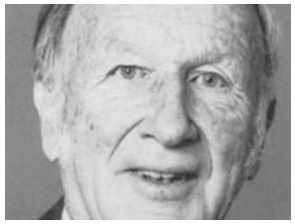

STUDIO DELLA STABILITA' DEL PUNTO FISSO:

X=-1.63…

Y=-1.63…

Z=1

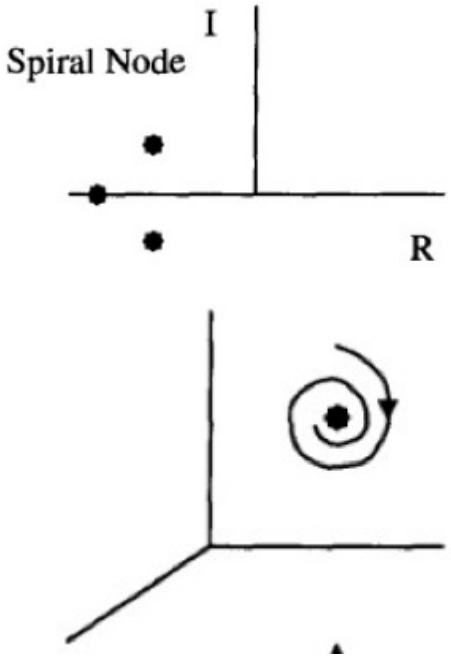

WolframAlpha computational knowledge engine

{{-p,p,0},{(r-z),-1,-x},{y,x,-b}} where p=10,b=8/3,r=2,x=-1.63,y=-1.63,z=1

Examples Random

r = 2

Input interpretation:

$$\begin{pmatrix} -p & p & 0 \\ r-z & -1 & -x \\ y & x & -b \end{pmatrix} \text{ where } p = 10,\ b = \frac{8}{3},\ r = 2,\ x = -1.63,\ y = -1.63,\ z = 1$$

Result:

$$\left\{\{-10,\ 10,\ 0\},\ \{1,\ -1,\ 1.63\},\ \left\{-1.63,\ -1.63,\ -\frac{8}{3}\right\}\right\}$$

Characteristic polynomial:

$$-x^3 - 13.6667\,x^2 - 31.9902\,x - 53.138$$

Eigenvalues:

$$\lambda_1 \approx -11.2414$$

$$\lambda_2 \approx -1.21263 + 1.80458\,i$$

$$\lambda_3 \approx -1.21263 - 1.80458\,i$$

Eigenvectors:

$$v_1 \approx (0.979108,\ -0.121548,\ 0.163016)$$

$$v_2 \approx (-0.370106 - 0.378644\,i,\ -0.256897 - 0.399518\,i,\ 0.702879 + 0.\,i)$$

$$v_3 \approx (-0.370106 + 0.378644\,i,\ -0.256897 + 0.399518\,i,\ 0.702879 + 0.\,i)$$

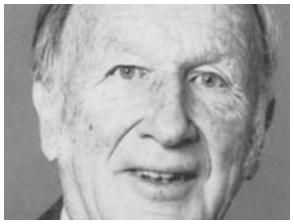

STUDIO DELLA STABILITA' DEL PUNTO FISSO:

X=1.63…

Y=1.63…

Z=1

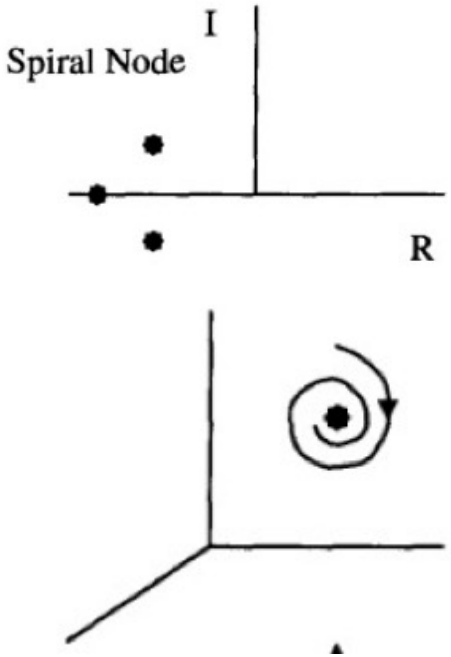

WolframAlpha computational… knowledge engine

{{-p,p,0},{(r-z),-1,-x},{y,x,-b}} where p=10,b=8/3,r=2,x=1.63,y=1.63,z=1

Examples Random

r = 2

Input interpretation:

$$\begin{pmatrix} -p & p & 0 \\ r-z & -1 & -x \\ y & x & -b \end{pmatrix} \text{ where } p = 10,\ b = \frac{8}{3},\ r = 2,\ x = 1.63,\ y = 1.63,\ z = 1$$

Result:

$$\left\{\{-10,\ 10,\ 0\},\ \{1,\ -1,\ -1.63\},\ \left\{1.63,\ 1.63,\ -\frac{8}{3}\right\}\right\}$$

Characteristic polynomial:

$$-x^3 - 13.6667\,x^2 - 31.9902\,x - 53.138$$

Eigenvalues:

$$\lambda_1 \approx -11.2414$$

$$\lambda_2 \approx -1.21263 + 1.80458\,i$$

$$\lambda_3 \approx -1.21263 - 1.80458\,i$$

Eigenvectors:

$$v_1 \approx (0.979108,\ -0.121548,\ -0.163016)$$

$$v_2 \approx (-0.370106 - 0.378644\,i,\ -0.256897 - 0.399518\,i,\ -0.702879 + 0.\,i)$$

$$v_3 \approx (-0.370106 + 0.378644\,i,\ -0.256897 + 0.399518\,i,\ -0.702879 + 0.\,i)$$

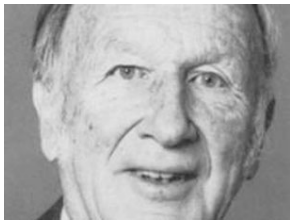

$$\begin{aligned}\dot{X} &= p(Y - X)\\ \dot{Y} &= -XZ + rX - Y\\ \dot{Z} &= XY - bZ\end{aligned}$$

p=10, b=8/3

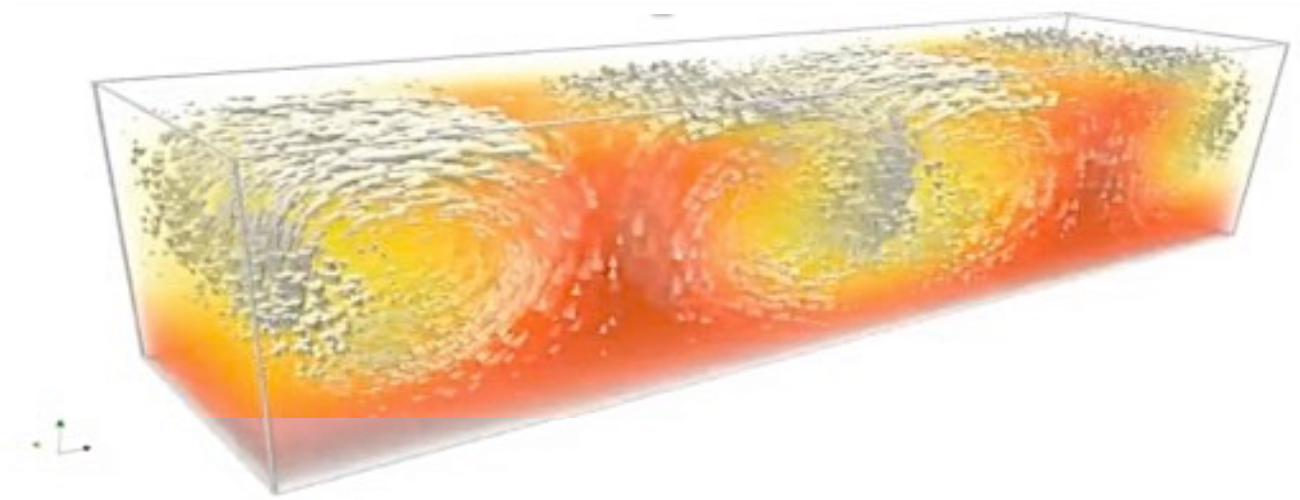

RIEPILOGO PARZIALE:

- **r < 1:** un unico **nodo** nell'origine.
- **1 < r < 13.93:** un **saddle point** (index 1) nell'origine + due **nodi a spirale** simmetrici off-origine.

Cosa succede per r > 13.93?

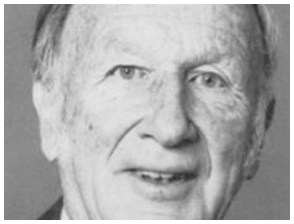

$$\begin{aligned}\dot{X} &= p(Y - X)\\ \dot{Y} &= -XZ + rX - Y\\ \dot{Z} &= XY - bZ\end{aligned}$$

p=10, b=8/3

14 circa < r < 25 circa

An interesting question to ask for any dynamical system is the following: What region of initial conditions in XYZ space leads to trajectories that go to each of the fixed points? In other words, what are the basins of attraction for the attracting fixed points? How do these regions change as the parameters describing the system change? We shall see later that these regions can be quite complicated geometrically. In fact, in order to describe them, we need to use the relatively new geometrical concept of ***fractals***. All of this, however, will be taken up in due course. Let us continue to increase the temperature difference for our fluid layer.

Nothing dramatic happens until r reaches about 13.93 where we find that repelling regions develop around the off-origin fixed points. There are still small basins of attraction surrounding the two off-origin fixed points, which give rise to trajectories attracted to those two points. Trajectories starting outside these small regions, however, are repelled from the vicinity of the fixed points. If we examine the graphs of $X(t)$, $Y(t)$, and $Z(t)$ shown in Fig. 1.19, then we see that the new conditions correspond to time dependent variations in the fluid flow and the corresponding temperature differences. The corresponding state space diagram is shown in the lower right of Fig. 1.19

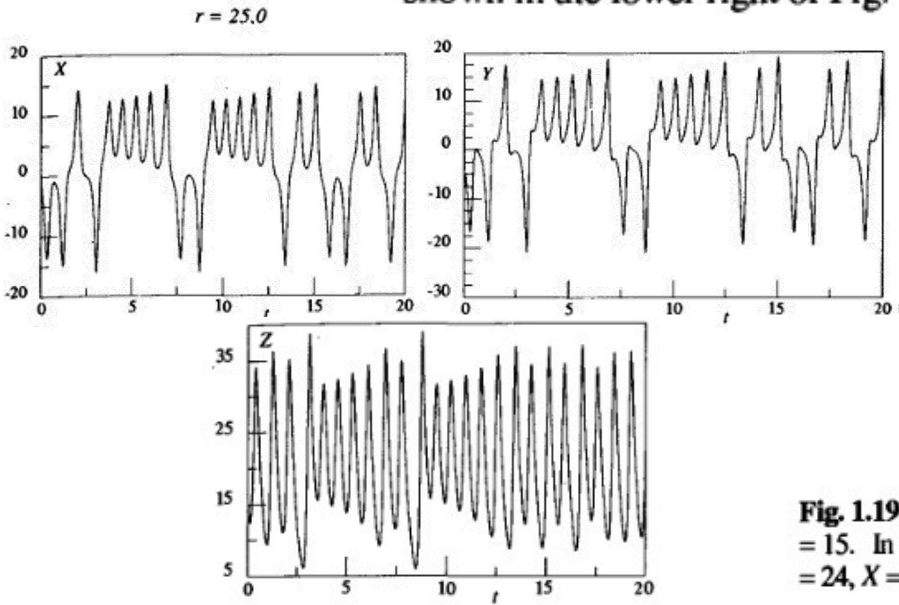

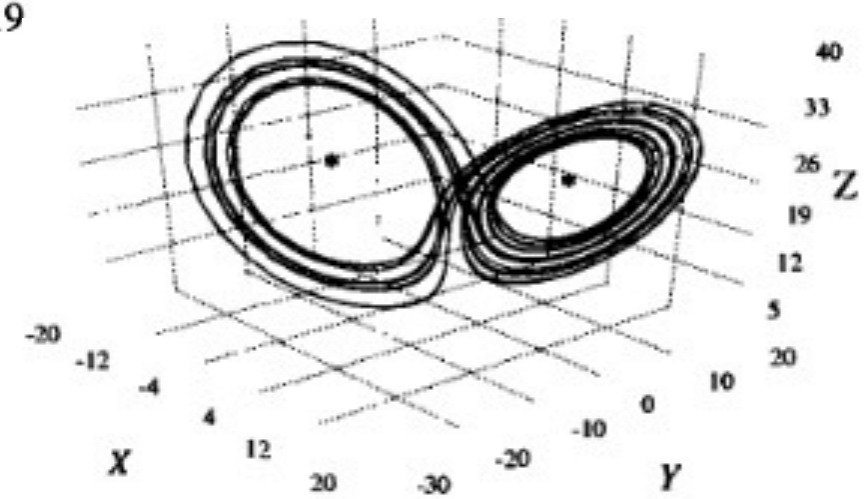

Fig. 1.19. Solutions to the Lorenz equations for $r = 25$. The initial point was $X = 0$, $Y = -5$, $Z = 15$. In the state space diagram in the lower right panel, the two off-origin fixed points at $Z = 24$, $X = 8$ and $Y = 8$ are indicated by asterisks.

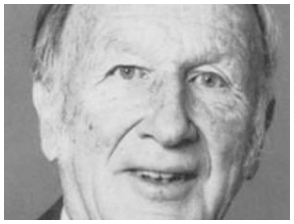

$$\dot{X} = p(Y - X)$$
$$\dot{Y} = -XZ + rX - Y$$
$$\dot{Z} = XY - bZ$$

p=10, b=8/3

r = 14

I due punti fissi off-origine restano nodi a spirale

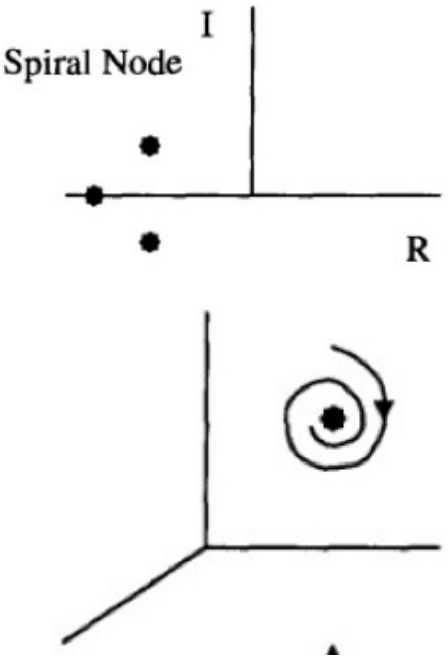

WolframAlpha computational intelligence

{{-p,p,0},{(r-z),-1,-x},{y,x,-b}} where p=10, b=8/3, r=14, x=sqrt(8/3)*sqrt(r-1),y=sqrt(8/3)*sqrt(r-1),z=r-1

NATURAL LANGUAGE | MATH INPUT | EXTENDED KEYBOARD | EXAMPLES | UPLOAD | RANDOM

Input interpretation

$$\begin{pmatrix} -p & p & 0 \\ r-z & -1 & -x \\ y & x & -b \end{pmatrix} \text{ where } p = 10, b = \frac{8}{3},$$
$$r = 14, x = \sqrt{\frac{8}{3}}\sqrt{r-1}, y = \sqrt{\frac{8}{3}}\sqrt{r-1}, z = r-1$$

Result

$$\begin{pmatrix} -10 & 10 & 0 \\ 1 & -1 & -2\sqrt{\frac{26}{3}} \\ 2\sqrt{\frac{26}{3}} & 2\sqrt{\frac{26}{3}} & -\frac{8}{3} \end{pmatrix}$$

Characteristic polynomial — Approximate form | Step-by-step solution

$$-\lambda^3 - \frac{41\lambda^2}{3} - 64\lambda - \frac{2080}{3}$$

Characteristic polynomial »

Eigenvalues — Exact forms | Step-by-step solution

$\lambda_1 \approx -12.8777$

$\lambda_2 \approx -0.394486 + 7.32695\,i$

$\lambda_3 \approx -0.394486 - 7.32695\,i$

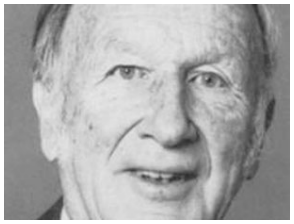

$$\dot{X} = p(Y - X)$$
$$\dot{Y} = -XZ + rX - Y$$
$$\dot{Z} = XY - bZ$$

p=10, b=8/3

r = 24

I due punti fissi off-origine restano nodi a spirale

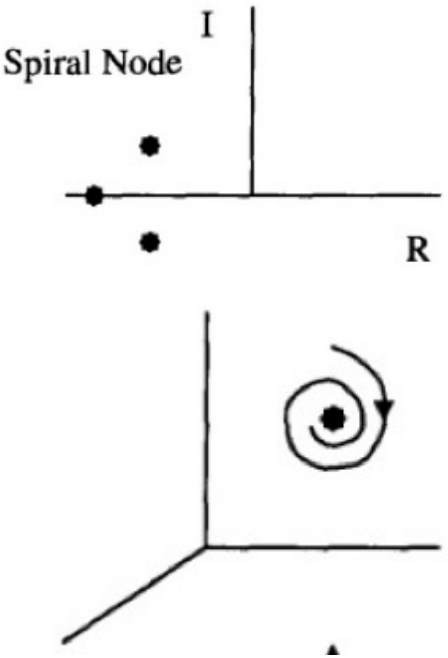

WolframAlpha computational intelligence

{{-p,p,0},{(r-z),-1,-x},{y,x,-b}} where p=10, b=8/3, r=24, x=sqrt(8/3)*sqrt(r-1),y=sqrt(8/3)*sqrt(r-1),z=r-1

NATURAL LANGUAGE | MATH INPUT | EXTENDED KEYBOARD | EXAMPLES | UPLOAD | RANDOM

Input interpretation

$$\begin{pmatrix} -p & p & 0 \\ r-z & -1 & -x \\ y & x & -b \end{pmatrix} \text{ where } p = 10, b = \frac{8}{3},$$
$$r = 24, x = \sqrt{\frac{8}{3}}\sqrt{r-1}, y = \sqrt{\frac{8}{3}}\sqrt{r-1}, z = r-1$$

Result

$$\begin{pmatrix} -10 & 10 & 0 \\ 1 & -1 & -2\sqrt{\frac{46}{3}} \\ 2\sqrt{\frac{46}{3}} & 2\sqrt{\frac{46}{3}} & -\frac{8}{3} \end{pmatrix}$$

Characteristic polynomial — Approximate form | Step-by-step solution

$$-\lambda^3 - \frac{41\lambda^2}{3} - \frac{272\lambda}{3} - \frac{3680}{3}$$

Characteristic polynomial »

Eigenvalues — Exact forms | Step-by-step solution

$$\lambda_1 \approx -13.6216$$
$$\lambda_2 \approx -0.0225267 + 9.4896\,i$$
$$\lambda_3 \approx -0.0225267 - 9.4896\,i$$

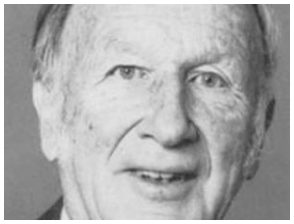

$$\begin{aligned}\dot{X} &= p(Y - X)\\ \dot{Y} &= -XZ + rX - Y\\ \dot{Z} &= XY - bZ\end{aligned}$$

p=10, b=8/3

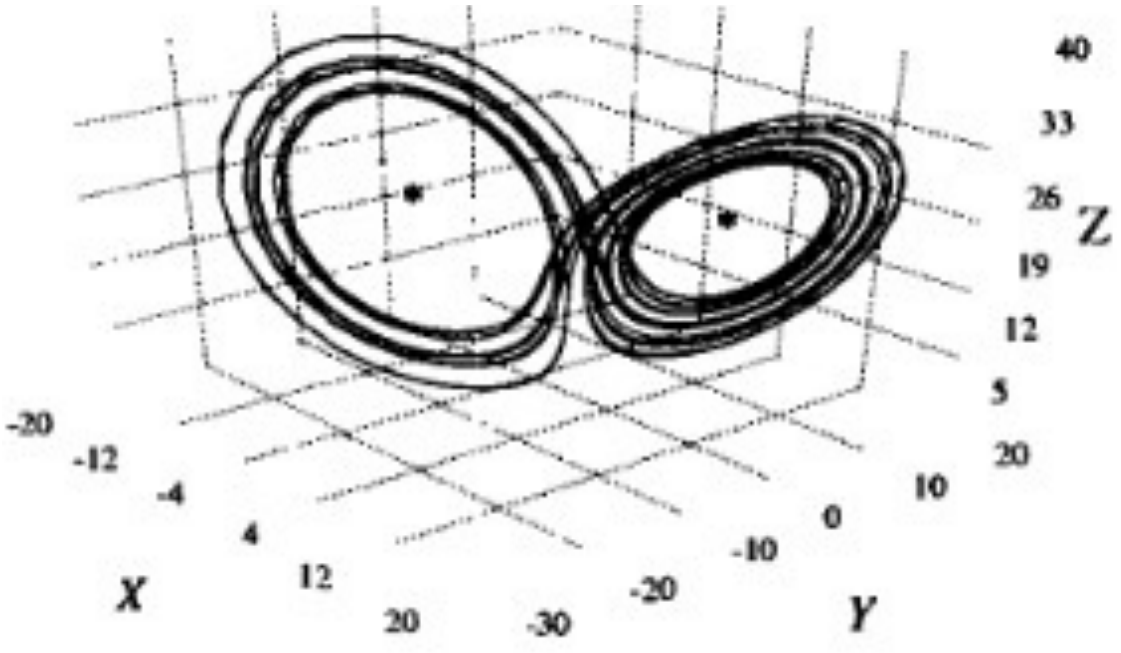

RIEPILOGO PARZIALE:

- **r < 1:** un unico **nodo** nell'origine.
- **1 < r < 13.93:** un **saddle point** (index 1) nell'origine + due **nodi a spirale** simmetrici off-origine.
- **13.93 < r < 24.74:** un **saddle point** (index 1) nell'origine + due **nodi a spirale** simmetrici off-origine + due **cicli limite saddle** (stabili all'interno, instabili all'esterno) attorno ai due nodi off-origine. Questi cicli limite diventano sempre più piccoli per r → 24.74.

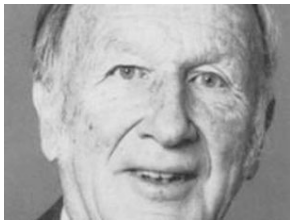

$$\begin{aligned}\dot{X} &= p(Y - X)\\ \dot{Y} &= -XZ + rX - Y\\ \dot{Z} &= XY - bZ\end{aligned}$$

p=10, b=8/3

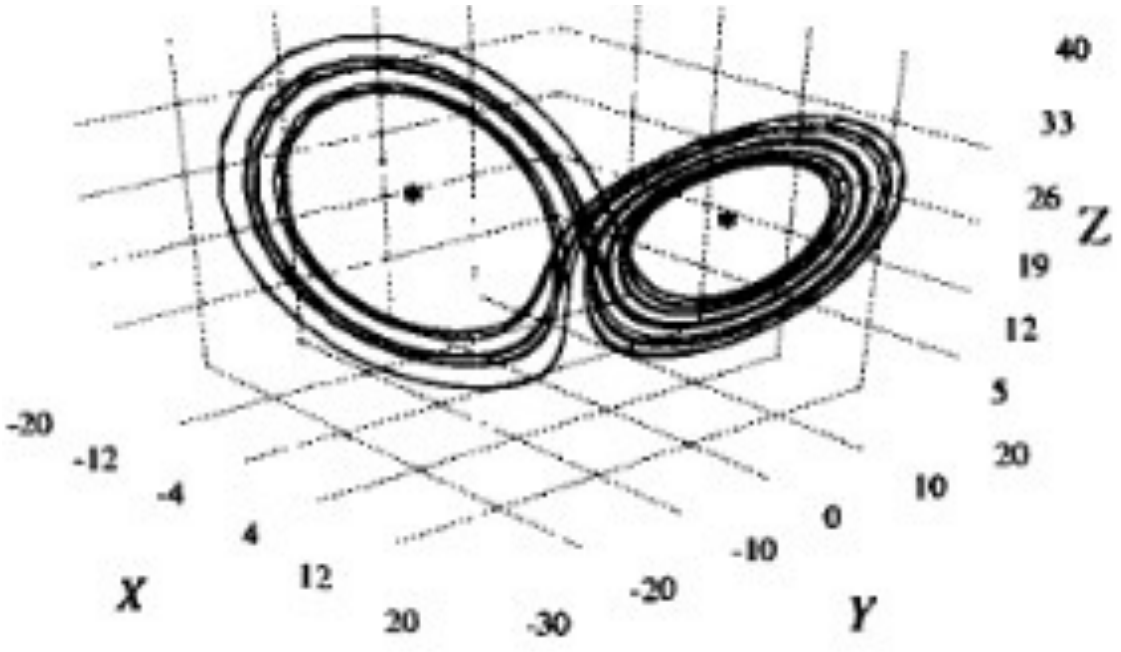

RIEPILOGO PARZIALE:

- **r < 1:** un unico **nodo** nell'origine.
- **1 < r < 13.93:** un **saddle point** (index 1) nell'origine + due **nodi a spirale** simmetrici off-origine.
- **13.93 < r < 24.74:** un **saddle point** (index 1) nell'origine + due **nodi a spirale** simmetrici off-origine + due **cicli limite saddle** (stabili all'interno, instabili all'esterno) attorno ai due nodi off-origine. Questi cicli limite diventano sempre più piccoli per r → 24.74.
- **r > 24.74:**

r =25

$x = -8, \quad y = -8, \quad z = 24$
$x = 0, \quad y = 0, \quad z = 0$
$x = 8, \quad y = 8, \quad z = 24$

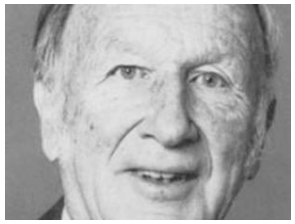

STUDIO DELLA STABILITA' DEL PUNTO FISSO:

X=0

Y=0

Z=0

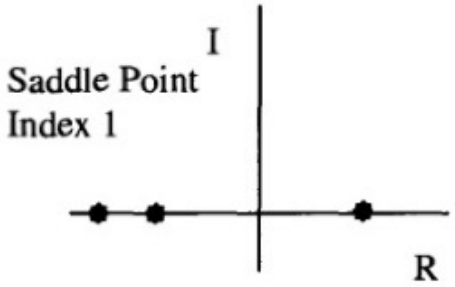

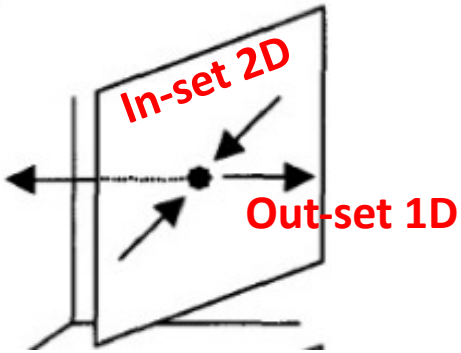

WolframAlpha computational... knowledge engine

{{-p,p,0},{(r-z),-1,-x},{y,x,-b}} where p=10,b=8/3,r=25,x=0,y=0,z=0

Examples Random

r = 25

Input interpretation:

$$\begin{pmatrix} -p & p & 0 \\ r-z & -1 & -x \\ y & x & -b \end{pmatrix} \text{ where } p = 10,\ b = \frac{8}{3},\ r = 25,\ x = 0,\ y = 0,\ z = 0$$

Result:

$$\left\{\{-10,\ 10,\ 0\},\ \{25,\ -1,\ 0\},\ \left\{0,\ 0,\ -\frac{8}{3}\right\}\right\}$$

Characteristic polynomial:

$$-x^3 - \frac{41\,x^2}{3} + \frac{632\,x}{3} + 640$$

Eigenvalues: Exact forms

$\lambda_1 \approx -21.9393$

$\lambda_2 \approx 10.9393$

$\lambda_3 \approx -2.66667$

Eigenvectors: Exact forms

$v_1 \approx (-0.837571,\ 1.,\ 0.)$

$v_2 \approx (0.477571,\ 1.,\ 0.)$

$v_3 \approx (0.,\ 0.,\ 1.)$

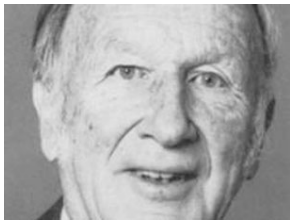

STUDIO DELLA STABILITA' DEL PUNTO FISSO:

X=-8

Y=-8

Z=24

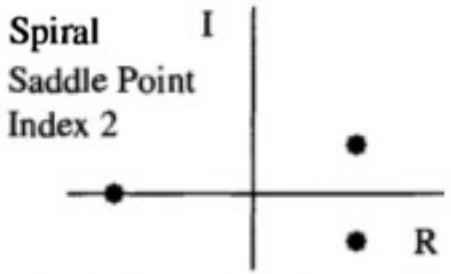

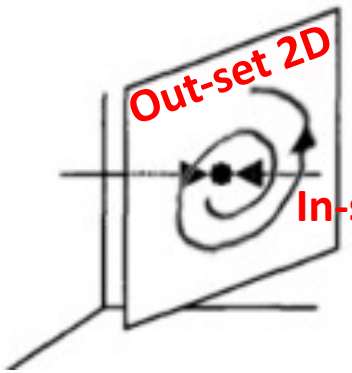

WolframAlpha computational knowledge engine

{{-p,p,0},{(r-z),-1,-x},{y,x,-b}} where p=10,b=8/3,r=25,x=-8,y=-8,z=24

Examples Random

r = 25

Input interpretation:

$$\begin{pmatrix} -p & p & 0 \\ r-z & -1 & -x \\ y & x & -b \end{pmatrix} \text{ where } p = 10,\ b = \frac{8}{3},\ r = 25,\ x = -8,\ y = -8,\ z = 24$$

Result:

$$\left\{\{-10,\ 10,\ 0\},\ \{1,\ -1,\ 8\},\ \left\{-8,\ -8,\ -\frac{8}{3}\right\}\right\}$$

Characteristic polynomial:

$$-x^3 - \frac{41\,x^2}{3} - \frac{280\,x}{3} - 1280$$

Eigenvalues: Exact forms

$\lambda_1 \approx -13.6825$

$\lambda_2 \approx 0.00792111 + 9.67213\,i$

$\lambda_3 \approx 0.00792111 - 9.67213\,i$

Eigenvectors: Exact forms

$v_1 \approx (2.17963,\ -0.802651,\ 1.)$

$v_2 \approx (-0.372223 - 0.42433\,i,\ 0.0378997 - 0.784685\,i,\ 1.)$

$v_3 \approx (-0.372223 + 0.42433\,i,\ 0.0378997 + 0.784685\,i,\ 1.)$

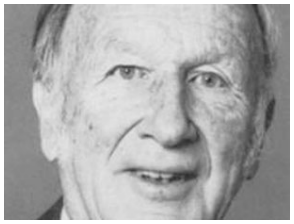

STUDIO DELLA STABILITA' DEL PUNTO FISSO:

X=8

Y=8

Z=24

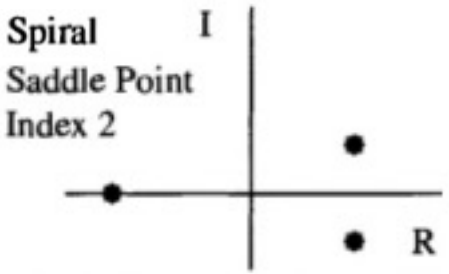

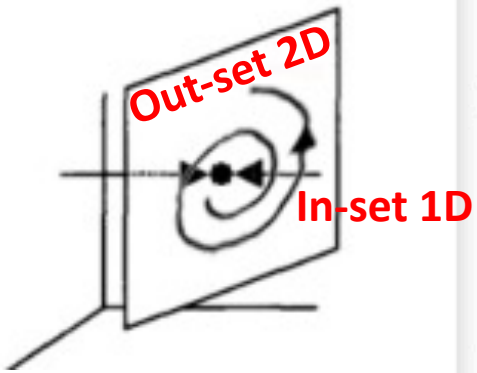

WolframAlpha computational knowledge engine

{{-p,p,0},{(r-z),-1,-x},{y,x,-b}} where p=10,b=8/3,r=25,x=8,y=8,z=24

Examples Random

r = 25

Input interpretation:

$$\begin{pmatrix} -p & p & 0 \\ r-z & -1 & -x \\ y & x & -b \end{pmatrix} \text{ where } p = 10,\ b = \frac{8}{3},\ r = 25,\ x = 8,\ y = 8,\ z = 24$$

Result:

$$\left\{\{-10,\ 10,\ 0\},\ \{1,\ -1,\ -8\},\ \left\{8,\ 8,\ -\frac{8}{3}\right\}\right\}$$

Characteristic polynomial:

$$-x^3 - \frac{41\,x^2}{3} - \frac{280\,x}{3} - 1280$$

Eigenvalues: Exact forms

$\lambda_1 \approx -13.6825$

$\lambda_2 \approx 0.00792111 + 9.67213\,i$

$\lambda_3 \approx 0.00792111 - 9.67213\,i$

Eigenvectors: Exact forms

$v_1 \approx (-2.17963,\ 0.802651,\ 1.)$

$v_2 \approx (0.372223 + 0.42433\,i,\ -0.0378997 + 0.784685\,i,\ 1.)$

$v_3 \approx (0.372223 - 0.42433\,i,\ -0.0378997 - 0.784685\,i,\ 1.)$

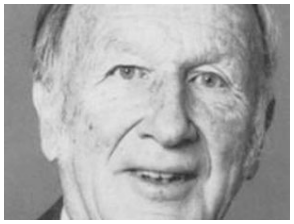

$$\begin{cases} \dot{X} = p(Y - X) \\ \dot{Y} = -XZ + rX - Y \\ \dot{Z} = XY - bZ \end{cases}$$

p=10, b=8/3

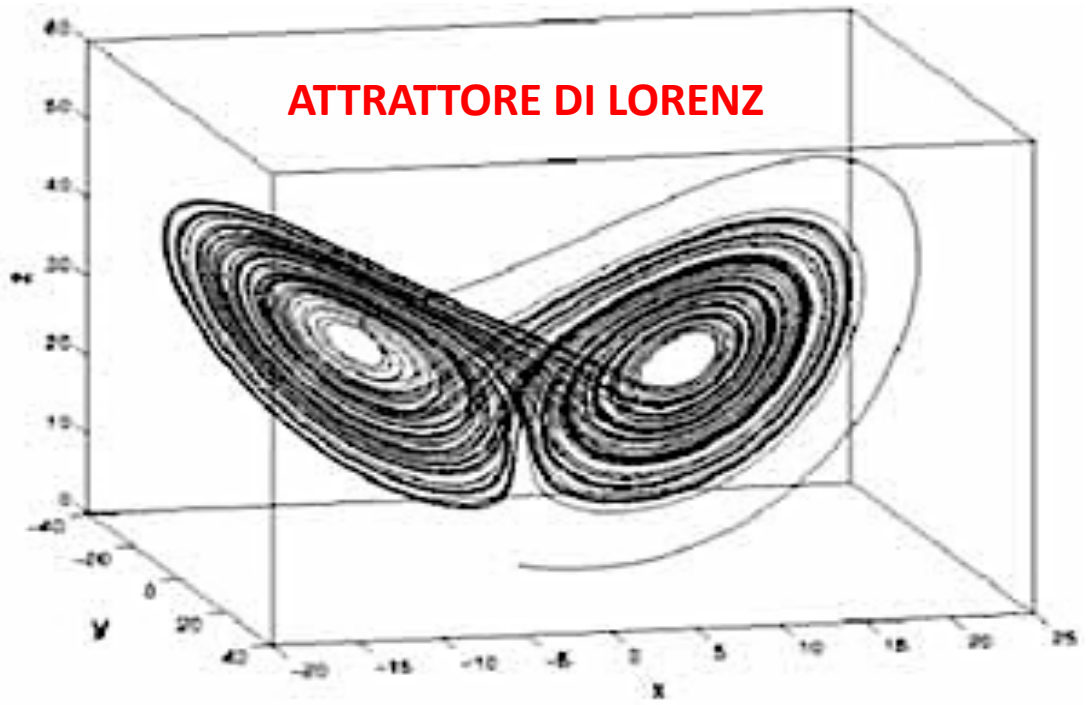

RIEPILOGO PARZIALE:

- **r < 1:** un unico **nodo** nell'origine.
- **1 < r < 13.93:** un **saddle point** (index 1) nell'origine + due **nodi a spirale** simmetrici off-origine.
- **13.93 < r < 24.74:** un **saddle point** (index 1) nell'origine + due **nodi a spirale** simmetrici off-origine + due **cicli limite saddle** (stabili all'interno, instabili all'esterno) attorno ai due nodi off-origine. Questi cicli limite diventano sempre più piccoli per r → 24.74.
- **r > 24.74:** un **saddle point** (index 1) nell'origine + due **saddle points** (index 2) a spirale simmetrici off-origine. I due cicli limite sono ormai collassati sui due punti fissi off-origine → **NASCE L'ATTRATTORE CAOTICO DI LORENZ**!!!

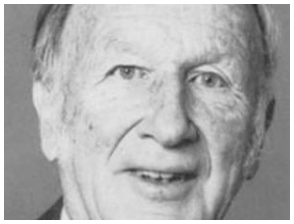

L'ATTRATTORE DI LORENZ POSSIEDE LE CARATTERISTICHE DEL COMPORTAMENTO CAOTICO

$$\dot{X} = p(Y - X)$$
$$\dot{Y} = -XZ + rX - Y$$
$$\dot{Z} = XY - bZ$$

p=10, b=8/3

r > 24.74

As we saw in Chapter 1, chaotic behavior is characterized by the divergence of nearby trajectories in state space. As a function of time, the "separation" (suitably defined) between two nearby trajectories increases exponentially, at least for short times. The last restriction is necessary because we are concerned with systems whose trajectories stay within some bounded region of state space. The system does not "blow up." There are three requirements for chaotic behavior in such a situation:

1. no intersection of different trajectories;
2. bounded trajectories;
3. exponential divergence of nearby trajectories.

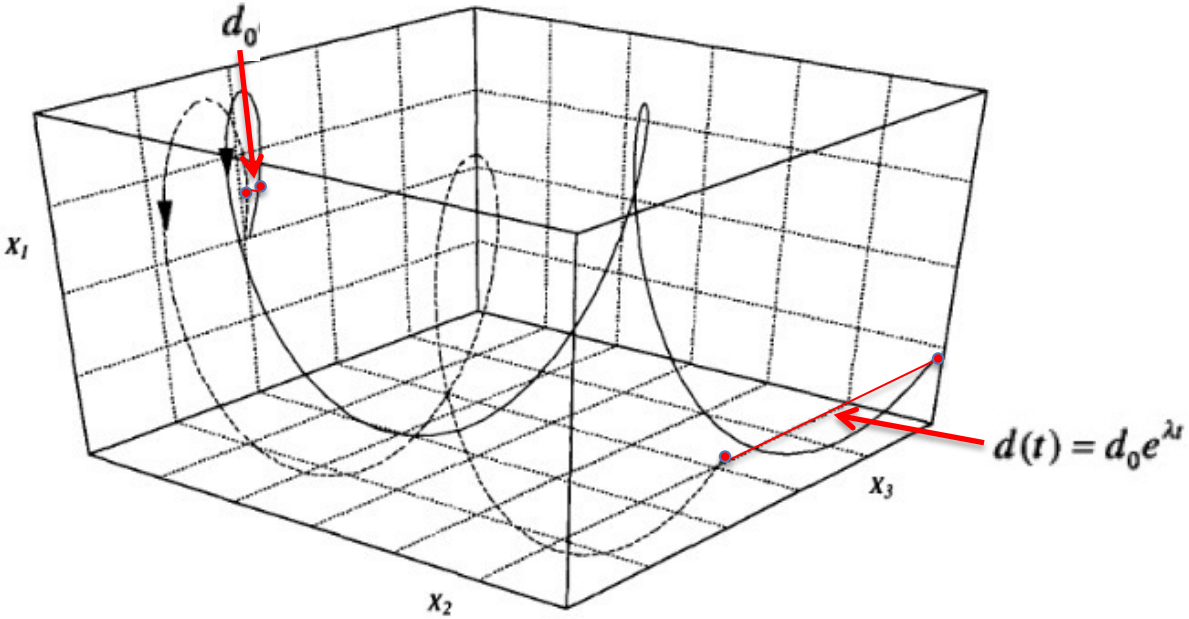

L'ATTRATTORE DI LORENZ POSSIEDE LE CARATTERISTICHE DEL COMPORTAMENTO CAOTICO

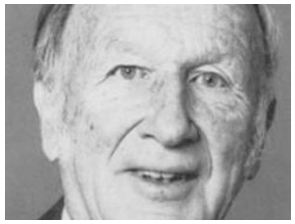

$$\dot{X} = p(Y - X)$$
$$\dot{Y} = -XZ + rX - Y$$
$$\dot{Z} = XY - bZ$$

p=10, b=8/3

r > 24.74

Chaos, however, also appears in the behavior of a single trajectory. As the trajectory wanders through the (chaotic) attractor in state space, it will eventually return near some point it previously visited. (Of course, it cannot return exactly to that point. If it did, then the trajectory would be periodic.) If the trajectories exhibit exponential divergence, then the trajectory on its second visit to a particular neighborhood will have subsequent behavior, quite different from its behavior on the first visit. Thus, the impression of the time record of this behavior will be one of nonreproducibility, nonperiodicity, in short, of chaos.

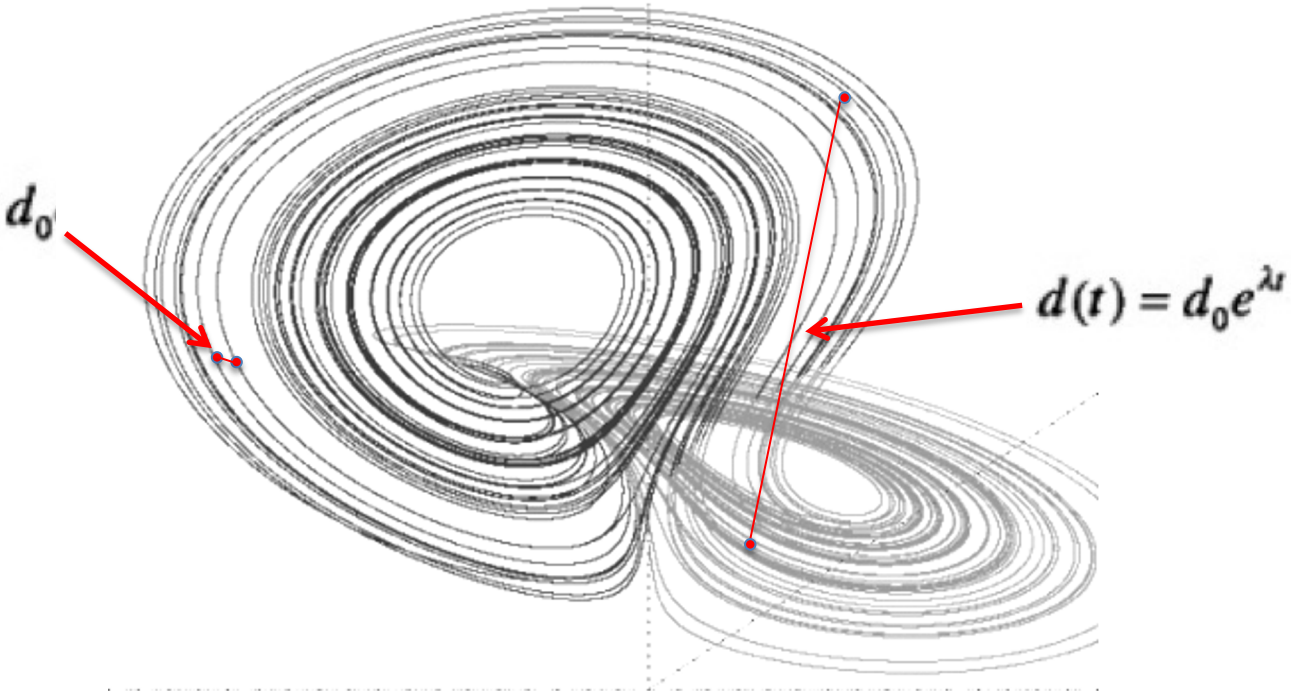

L'ATTRATTORE DI LORENZ POSSIEDE LE CARATTERISTICHE DEL COMPORTAMENTO CAOTICO

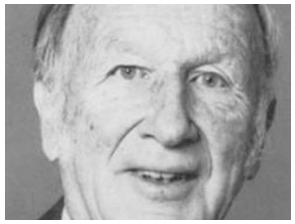

$$\dot{X} = p(Y - X)$$
$$\dot{Y} = -XZ + rX - Y$$
$$\dot{Z} = XY - bZ$$

p=10, b=8/3

r > 24.74

This observation should be the cause of some reflection. Here, we have a system for which the externally controlled "forcing" (that is, the imposed temperature difference) is independent of time. Yet the system has developed spontaneously a nontrivial time dependence. As we mentioned before, a nonlinear system can break the time-translation symmetry of its fundamental equations and external environment. (The period-2, period-4, and so on, variations of populations in the logistic map model are also examples of the spontaneous breaking of time-translation symmetry.)

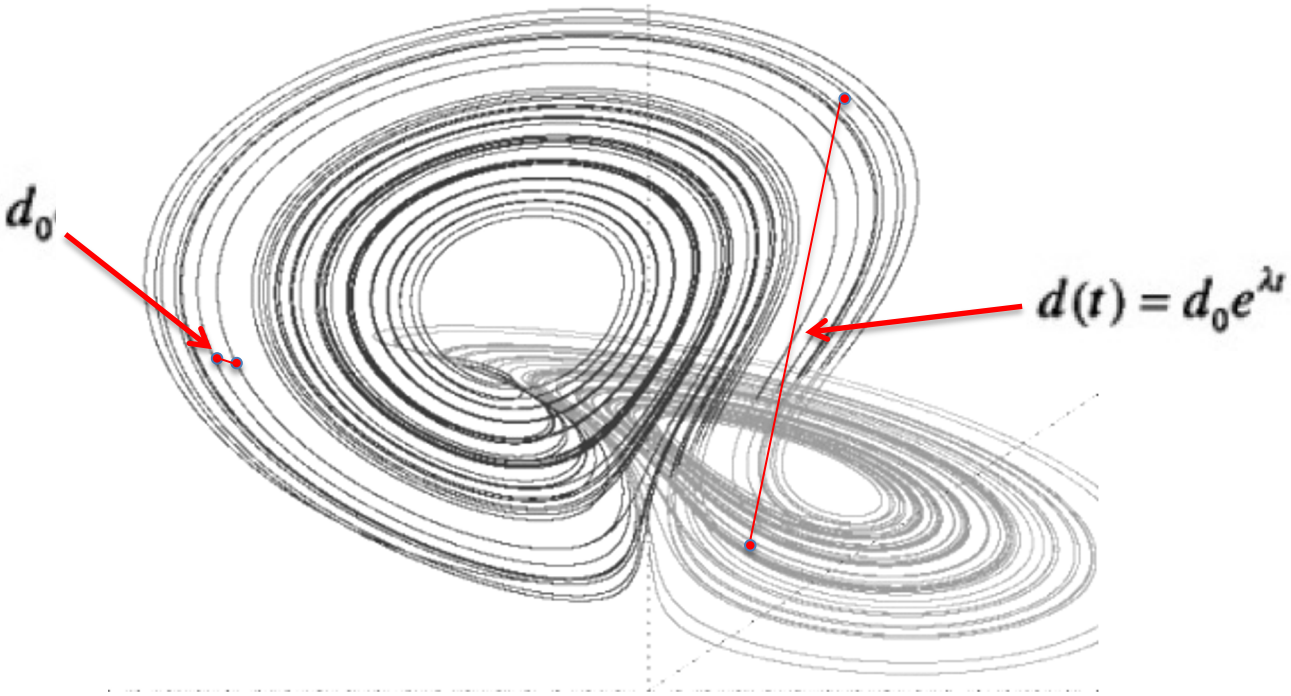

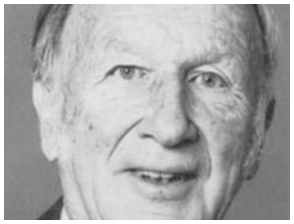

$$\begin{aligned}\dot{X} &= p(Y - X)\\ \dot{Y} &= -XZ + rX - Y\\ \dot{Z} &= XY - bZ\end{aligned}$$

p=10, b=8/3

MA QUAL'E' LA ROTTA CHE CONDUCE ALL'ATTRATTORE CAOTICO DI LORENZ PER r -> 24.74?

Dobbiamo guardare cosa succedeva dietro le quinte mentre aumentavamo il valore di r...

r < 1

↓

r > 1

↓

r > 13.93

↓

r > 24.74

CAOS!

?

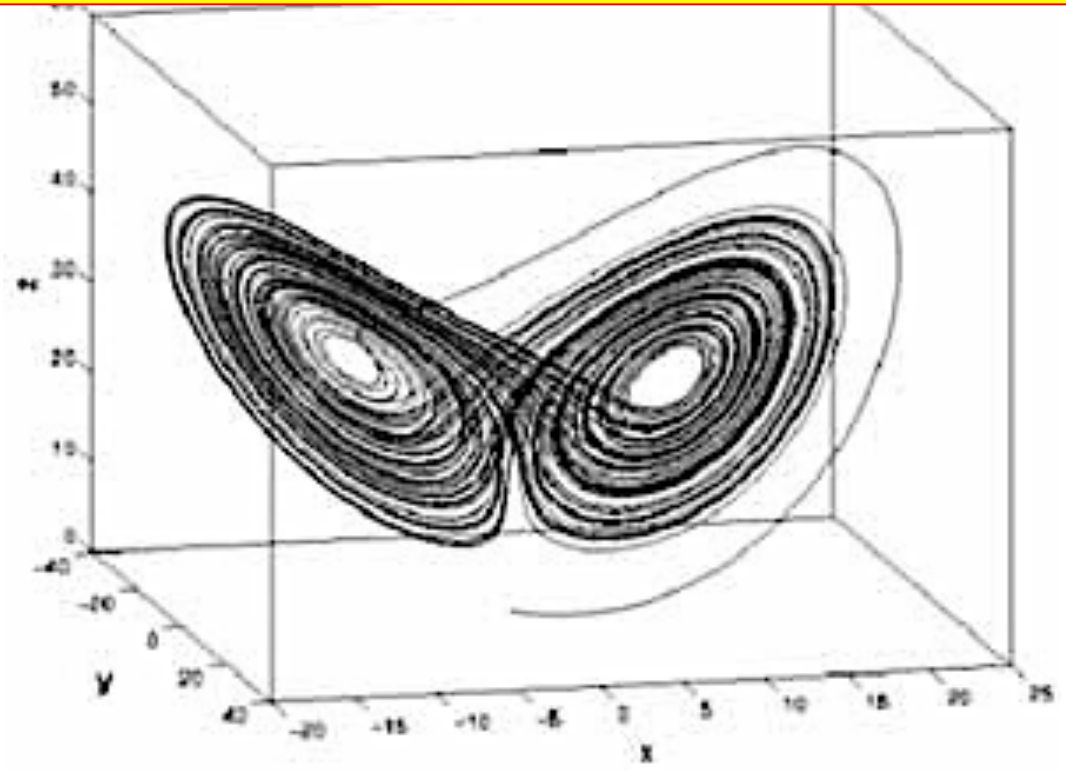

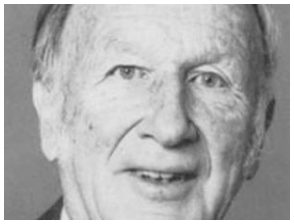

$$\dot{X} = p(Y - X)$$
$$\dot{Y} = -XZ + rX - Y$$
$$\dot{Z} = XY - bZ$$

p=10, b=8/3

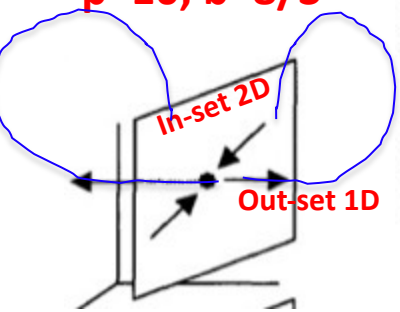

Saddle Point
Index 1
(0,0,0)

The Routes to Chaos IV: Chaotic Transients and Homoclinic Orbits

As an example of how homoclinic and heteroclinic connections affect dynamics, let us return to the Lorenz model introduced in Chapter 1. This model provides a nice example of chaotic transients due to homoclinic and heteroclinic connections eventually leading to chaotic behavior. A homoclinic connection is formed when the parameter r is near 13.93 (with $b = 8/3$ and $p = 10$, as in Chapter 1). At that parameter value, the one-dimensional out-set of the fixed point at the origin, which is now a saddle point, touches, over its entire length, the two-dimensional in-set of that same saddle point. Actually, a double homoclinic connection is formed because there are two branches of the one-dimensional out-set, one leading to one of the off-origin fixed points, the other leading to the other off-origin fixed point. Trajectories passing near the homoclinic connections are successively repelled by and attracted to the saddle point at the origin many times while wandering back and forth between regions around the two off-origin fixed points before finally settling into one of the off-origin fixed points. Such behavior looks chaotic, but because it is really only transient behavior, it is called ***transient chaos***. For more information about transient chaos, a fascinating topic in its own right, see the references at the end of this chapter.

1 < r < 13.93: un **saddle point** (index 1) nell'origine + due **nodi a spirale** simmetrici off-origine.

DOPPIA CONNESSIONE OMOCLINICA DEL SADDLE POINT NELL'ORIGINE CON SE STESSO per r=13.93…

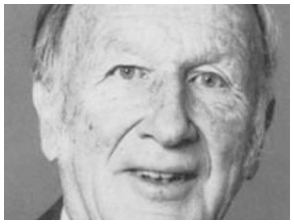

$$\begin{aligned}\dot{X} &= p(Y - X)\\ \dot{Y} &= -XZ + rX - Y\\ \dot{Z} &= XY - bZ\end{aligned}$$

p=10, b=8/3

When this homoclinic connection occurs, two saddle cycles are also created. These saddle cycles play an essential role in the development of the chaotic attractor in the Lorenz model. As r increases beyond 13.93, the saddle cycles, which surround the off-origin fixed points (which themselves are spiral nodes), begin to decrease in size and contract around the spiral nodes. At $r = 24.74$, the real part of the complex eigenvalues of the spiral nodes goes to 0, and the saddle cycles collapse onto the nodes. Before this, however, at $r < 24.06$, the out-set of the saddle point at the origin falls outside the saddle cycles. For $r > 24.06$ the out-set falls inside the saddle cycles; therefore, at $r = 24.06$ (approximately), the out-set of the saddle point at the origin must intersect the saddle cycles to form a heteroclinic connection. For $r < 24.74$, there are still two (small) basins of attraction near the two spiral nodes, but trajectories starting outside these two small basins wander chaotically due to the influence of the heteroclinic connection and resulting tangle. In effect, a chaotic attractor has been formed by this connection. Figure 4.17 shows how the resulting heteroclinic connections influence a trajectory that starts near the saddle point at the origin.

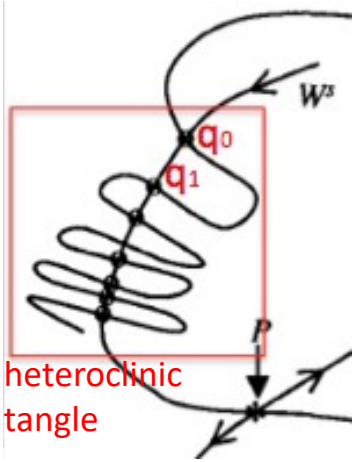

heteroclinic tangle

r > 13.93: nascono due **cicli limite saddle** (instabili all'esterno) attorno ai due nodi off-origine

…E DOPPIA CONNESSIONE ETEROCLINICA CON I DUE SADDLE CYCLE OFF-ORIGINE per r=24.06

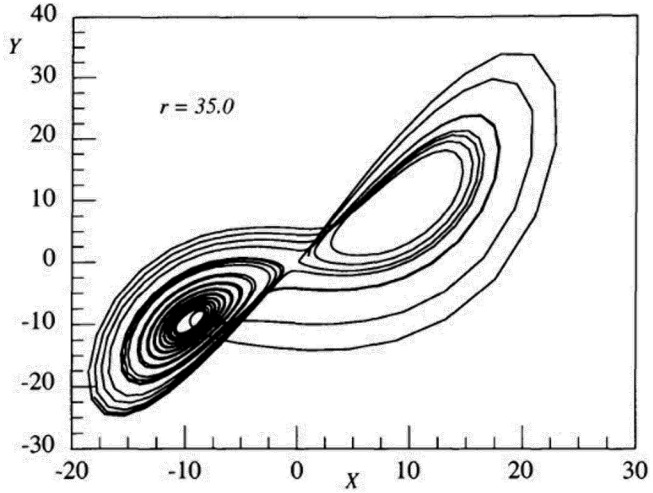

Fig. 4.17. An illustration of heteroclinic behavior in the Lorenz model at $r = 35.0$. The XY plane projection of the trajectory is shown. The trajectory starts near the saddle point at the origin. The out-set of the origin connects to the in-set of one of the saddle cycles near the fixed point at $X = Y = +9.5$. The trajectory then leaves that saddle cycle on its out-set which connects to the in-set of the other saddle cycle. After orbiting near the fixed point at $X = Y = -9.5$, the trajectory heads back toward the origin on the out-set of the saddle cycle. Near the origin, it is again repelled.

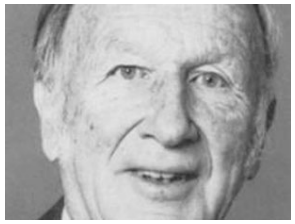

RIEPILOGO
QUASI FINALE...

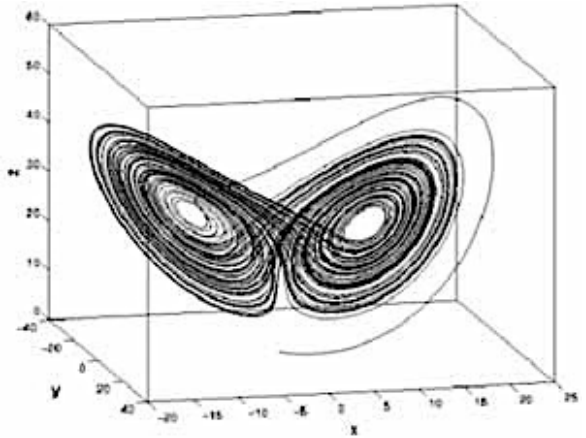

- **r < 1:** un unico **nodo** nell'origine.
- **1 < r < 13.93:** un **saddle point** (index 1) nell'origine + due **nodi a spirale** simmetrici off-origine.
- **r = 13.93: doppia connessione omoclinica** tra i due rami dell'out-set (1Dim) del saddle point nell'origine e il suo stesso in-set (2Dim) – **TRANSIENT CHAOS**
- **13.93 < r < 24.74:** un **saddle point** (index 1) nell'origine + due **nodi a spirale** simmetrici off-origine + due **cicli limite saddle** (stabili all'interno, instabili all'esterno) attorno ai due nodi off-origine. Questi cicli limite diventano sempre più piccoli per r → 24.74.
- **r = 24.06:** i due rami dell'out-set (1Dim) del **saddle point** nell'origine formano una **doppia connessione eteroclinica** con gli in-set (2D) dei cicli limite saddle attorno ai due punti fissi off-origine. Si forma **l'ATTRATTORE CAOTICO** di Lorenz.
- **r > 24.74:** un **saddle point** (index 1) nell'origine + due **saddle points** (index 2) a spirale simmetrici off-origine. I due cicli limite sono ormai collassati sui due punti fissi off-origine.
- **24.74 < r < 143:** comportamento **CAOTICO.**

Cosa succede per r > 143?

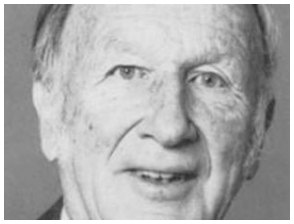

«PERIOD DOUBLING ROUTE» VERSO L'ATTRATTORE DI LORENZ

$$\dot{X} = p(Y - X)$$
$$\dot{Y} = -XZ + rX - Y$$
$$\dot{Z} = XY - bZ$$

p=10, b=8/3

r = 160

The time behavior in this region of r values is quite complex. So let us move on to examine another region near $r = 160$. Figure 1.20 shows the time dependence of X, Y, and Z for $r = 160$. The behavior is not simple harmonic (that is, it is not sinusoidal), but it is periodic. We can understand the physical nature of the system's behavior by looking at the graphs of X and Y as functions of time. We see that X oscillates symmetrically around the value $X = 0$. This tells us that the fluid is convecting first in the clockwise direction, then counterclockwise, continually reversing as time goes on. The temperature difference between up flow and down flow, represented by the variable Y, also oscillates symmetrically around 0. Note that the Z variable, on the other hand, oscillates around a nonzero value (approximately 160 for the case displayed in Fig. 1.20).

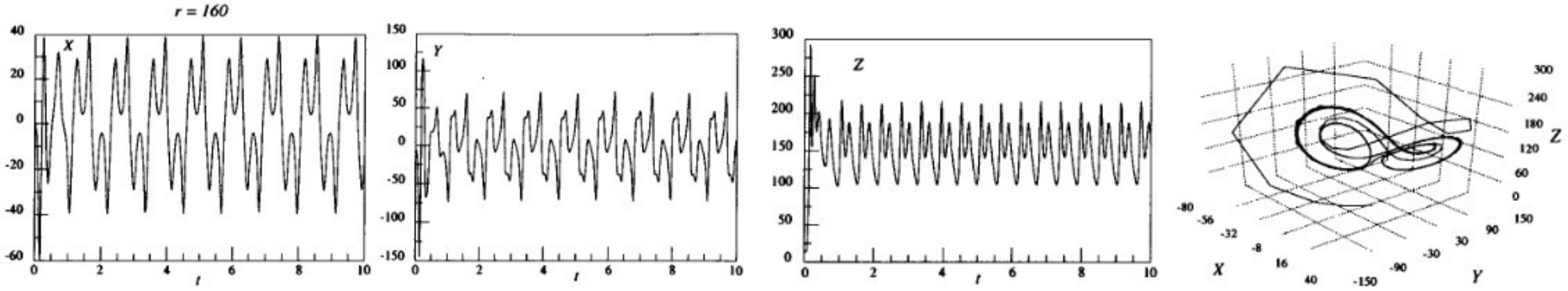

Fig. 1.20. Solutions of the Lorenz equations with $r = 160$. After an initial transient that lasts until about $t = 3$, the solutions are periodic (but not sinusoidal). The jaggedness of the transient trajectory in the XYZ state space plot (lower right) is a graphing artifact. The calculations were actually carried out with much smaller time steps.

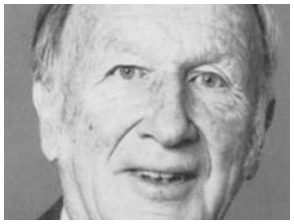

$$\dot{X} = p(Y - X)$$
$$\dot{Y} = -XZ + rX - Y$$
$$\dot{Z} = XY - bZ$$

p=10, b=8/3

When the Rayleigh number is decreased to about $r = 150$, we find that the periodic behavior of Z suddenly changes. Figure 1.21 indicates that we now have period-2 behavior. (Please note a complication: The fundamental period is also slightly changed from Fig. 1.20. The Lorenz model does not have any external periodic forcing, as did the diode circuit, to determine the fundamental period.) The period-2 behavior is most easily recognized by looking at the largest upward "peaks" or downward "troughs" in Fig. 1.21. We see that a period-doubling bifurcation has occurred.

At $r \approx 146$, we find that $Z(t)$ bifurcates again, now with a period four times the original. [Similar, but less dramatic changes occur in $Y(t)$ and $X(t)$.] As r decreases below about 144, the behavior of all the variables becomes completely aperiodic. We have seen yet another period-doubling route to chaos. (We have not generated a complete bifurcation diagram for this range of r values because of the amount of computation time involved.)

r = 160
↓
r = 150
↓
r = 146
↓
r = ...

PERIOD DOUBLING

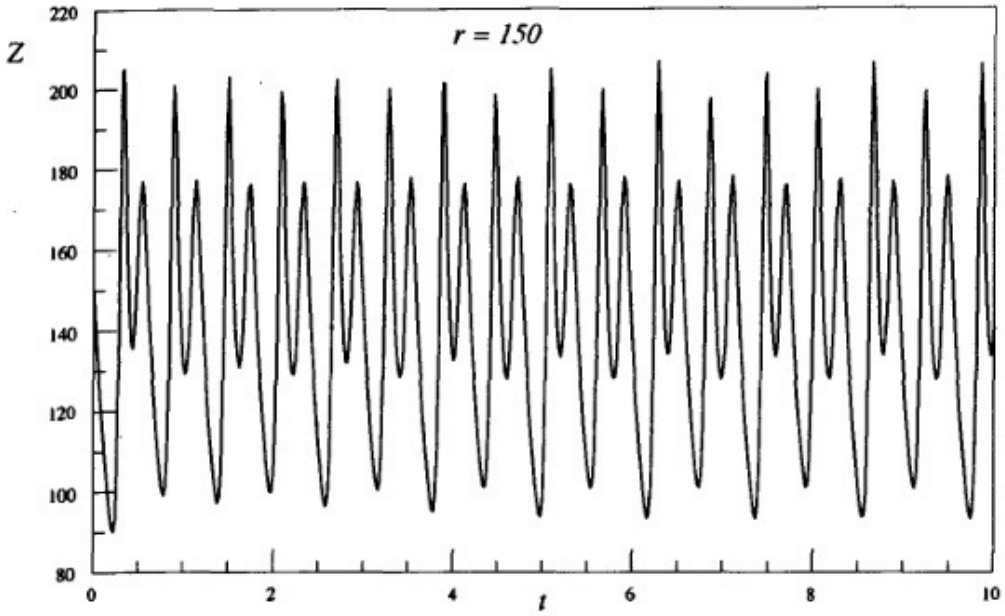

Fig. 1.21. $Z(t)$ for the Lorenz equations with $r = 150$. After an initial transient, the behavior is periodic with a period twice that seen in Fig. 1.20. Notice the alternating heights of the largest peaks in this figure.

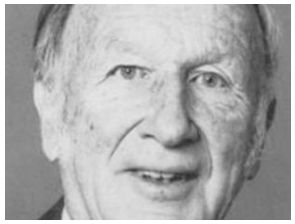

Attrattore Caotico di Lorenz

(Dim.Frattale D=2.06 ± 0.01)

$$\begin{aligned}\dot{X} &= p(Y - X)\\ \dot{Y} &= -XZ + rX - Y\\ \dot{Z} &= XY - bZ\end{aligned}$$

p=10, b=8/3

r = 160

↓

r = 150

↓

r = 146

↓

r = 143

CAOS!

PERIOD DOUBLING

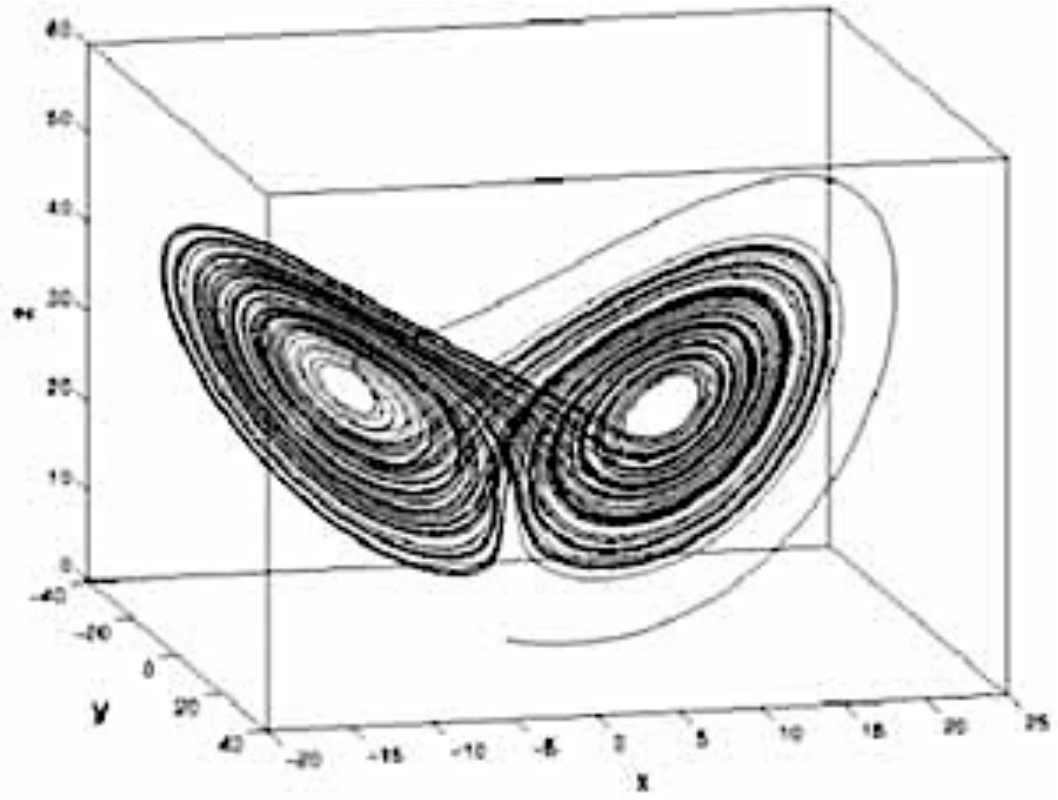

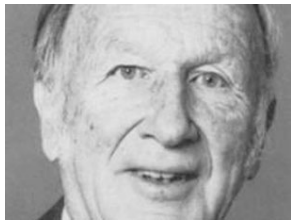

$$\dot{X} = p(Y - X)$$
$$\dot{Y} = -XZ + rX - Y$$
$$\dot{Z} = XY - bZ$$

p=10, b=8/3

r = 160

↓

r = 150

↓

r = 146

↓

r = 143

CAOS!

PERIOD DOUBLING

Divergence of Trajectories in the Lorenz Model

We now want to address the crucial question in deciding whether or not the Lorenz model equations exhibit chaotic behavior for some range of r values: Do nearby trajectories diverge for that range of r values? Figure 1.22 shows two trajectories for $r = 143$ with slightly different initial conditions. We see that after only a few oscillations the trajectories are completely different. Although this result does not prove the existence of the divergence of nearby trajectories on the average, it does suggest that the Lorenz model displays chaotic behavior for $r = 143$.

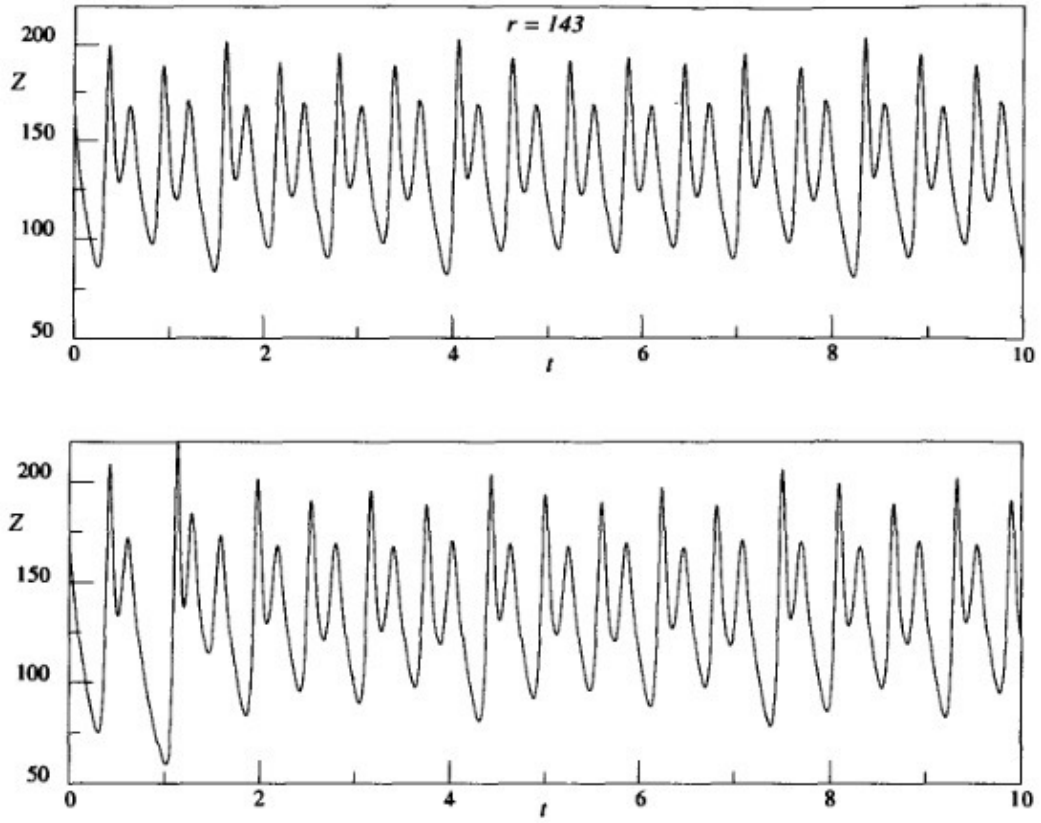

Fig. 1.22. Two trajectories in the Lorenz model showing divergence of nearby trajectories for $r = 143$. The trajectory in the upper panel starts with the initial conditions $X = 20$, $Y = 0$, $Z = 163$. In the lower panel the nearby trajectory starts with $X = 20$, $Y = 0$, $Z = 166$. After only a few oscillations the trajectories are completely different.

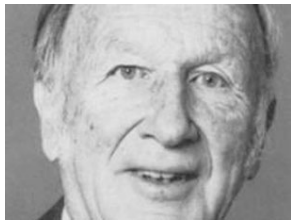

RIEPILOGO FINALE

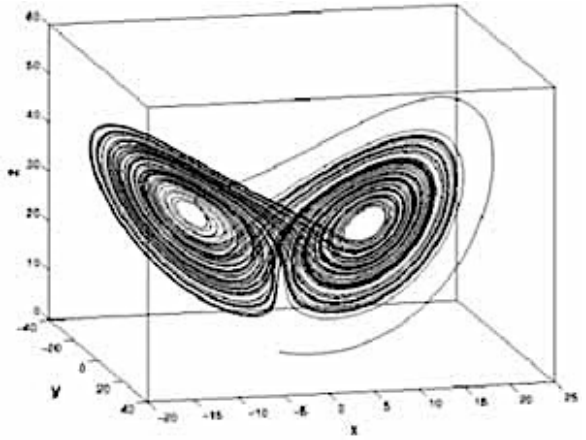

- **r < 1:** un unico **nodo** nell'origine.
- **1 < r < 13.93:** un **saddle point** (index 1) nell'origine + due **nodi a spirale** simmetrici off-origine.
- **r = 13.93: doppia connessione omoclinica** tra i due rami dell'out-set (1Dim) del saddle point nell'origine e il suo stesso in-set (2Dim) – **TRANSIENT CHAOS**
- **13.93 < r < 24.74:** un **saddle point** (index 1) nell'origine + due **nodi a spirale** simmetrici off-origine + due **cicli limite saddle** (stabili all'interno, instabili all'esterno) attorno ai due nodi off-origine. Questi cicli limite diventano sempre più piccoli per r → 24.74.
- **r = 24.06:** i due rami dell'out-set (1Dim) del **saddle point** nell'origine formano una **doppia connessione eteroclinica** con gli in-set (2D) dei cicli limite saddle attorno ai due punti fissi off-origine. Si forma **l'ATTRATTORE CAOTICO** di Lorenz.
- **r > 24.74:** un **saddle point** (index 1) nell'origine + due **saddle points** (index 2) a spirale simmetrici off-origine. I due cicli limite sono ormai collassati sui due punti fissi off-origine.
- **24.74 < r < 143:** comportamento **CAOTICO.**
- **r: 160 -> 143 :** sequenza di **raddoppiamenti di periodo** nei cicli limite attrattivi che si sviluppano attorno ai due punti fissi off-origine.

4.12 Homoclinic Tangles and Horseshoes

Stephen Smale

A very elegant and useful geometric model of the effect of homoclinic and heteroclinic tangles on state-space orbits is the Smale horseshoe. This equestrian metaphor was introduced by the mathematician Stephen Smale (SMA67) to capture the essence of the effects of homoclinic tangles on dynamical systems. The horseshoe construction has the additional benefit of providing a scheme that allows mathematical proofs of many important aspects of the dynamics of the system. We shall introduce the basic horseshoe idea here. In Chapter 5, we will take up the mathematical results from this construction.

To understand Smale's construction, let us consider a small rectangle of initial points surrounding a saddle point in the Poincaré section of a dynamical system. As the system evolves, this rectangle of points will tend to be stretched out along the unstable manifold direction W^u and compressed along the W^s direction. The rectangle will eventually reach the tangled region of W^u shown in Fig. 4.13, and its shape will resemble a horseshoe. As the system evolves further, this horseshoe will in fact eventually overlap with the original rectangle. Smale constructed a mapping function, now known as the Smale horseshoe map, which captures the essence of this process.

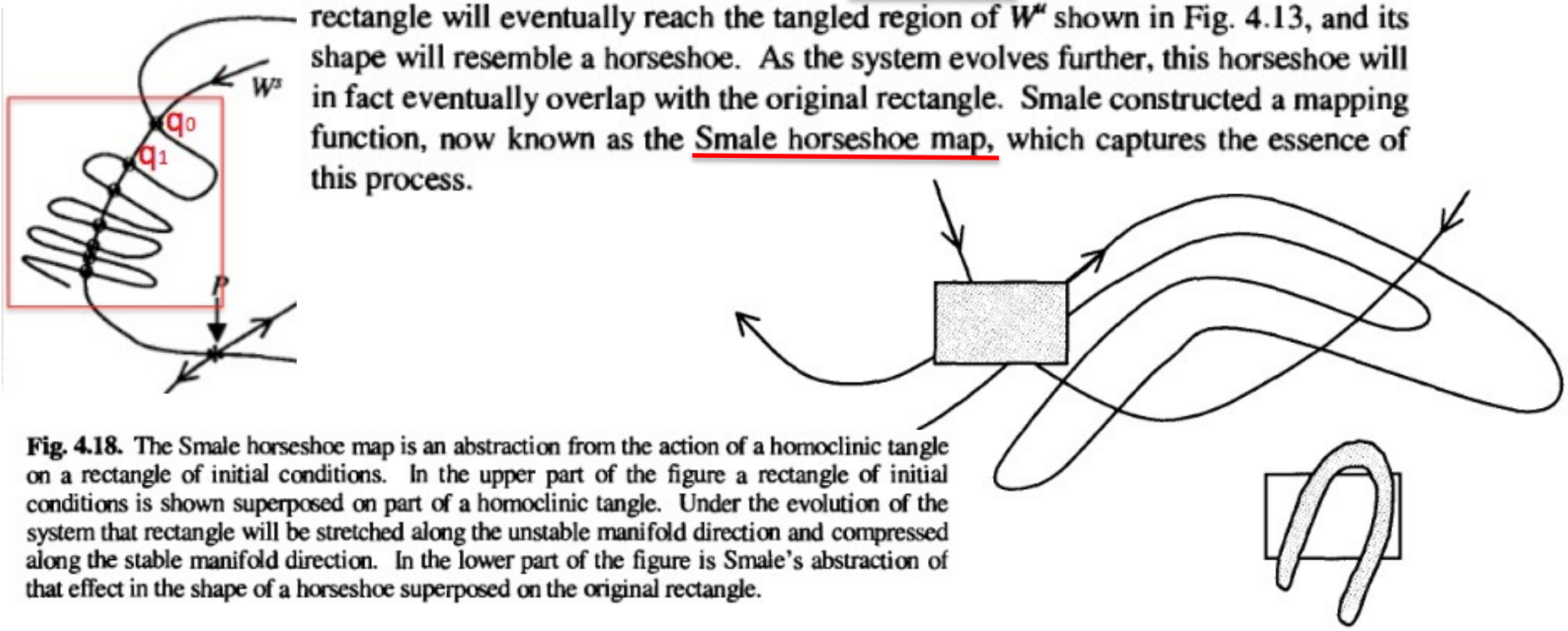

Fig. 4.18. The Smale horseshoe map is an abstraction from the action of a homoclinic tangle on a rectangle of initial conditions. In the upper part of the figure a rectangle of initial conditions is shown superposed on part of a homoclinic tangle. Under the evolution of the system that rectangle will be stretched along the unstable manifold direction and compressed along the stable manifold direction. In the lower part of the figure is Smale's abstraction of that effect in the shape of a horseshoe superposed on the original rectangle.

Stephen Smale

In the Smale horseshoe map, a square of initial points is first stretched in one direction and compressed in the orthogonal direction. The now elongated rectangle is folded and overlaid on the initial square (see Fig. 4.18). The process is iterated, and one looks for those points that remain within the area of the initial square as the number of iterations goes to infinity. This stretching in one direction, compressing in another, combined with the folding, mimics the effect of the homoclinic tangle on trajectories in the dynamical system. The famous Smale–Birkhoff Homoclinic Theorem proves [Guckenheimer and Holmes, 1990] that having a homoclinic tangle guarantees that the system will have "horseshoe dynamics."

Stretching, Compression and Folding

Although the original Smale horseshoe map does not have an attractor and hence cannot be a model for the chaotic behavior of a dissipative system, many authors have decided to equate chaotic behavior with horseshoe dynamics because the stretching (in at least one state space direction) gives rise to exponential divergence of nearby initial conditions. Certainly in the general sense of requiring stretching in one direction, compression in another, combined with folding to keep the system in

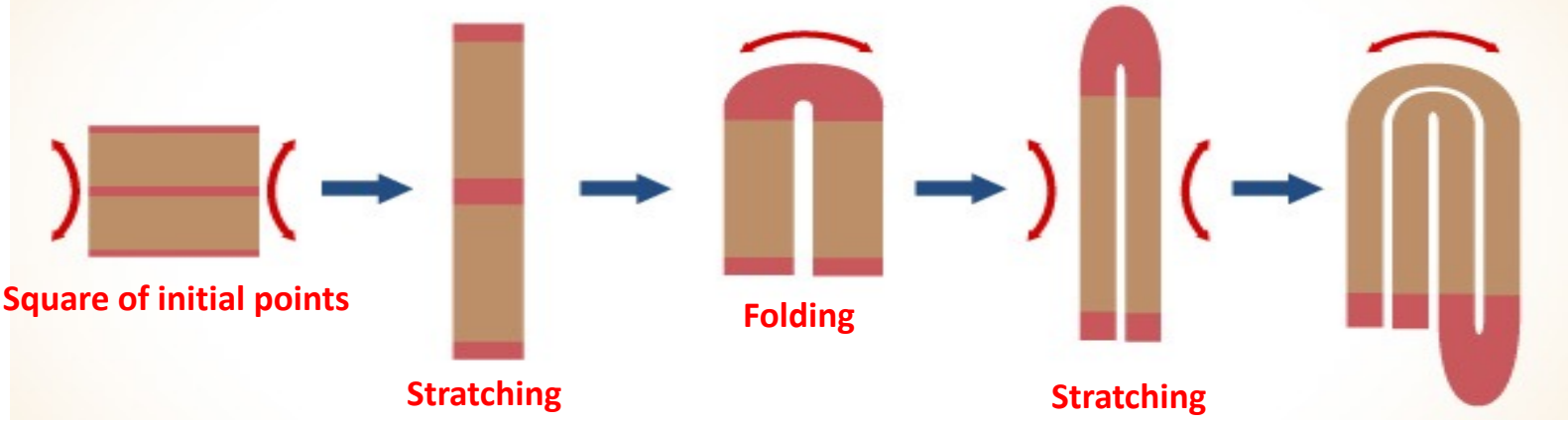

Stephen Smale

a finite region of state space, horseshoe dynamics must be a general feature of all chaotic behavior.

As mentioned earlier, in many systems the stretching and folding is actually effected by heteroclinic connections, which link the unstable manifold of one saddle cycle (in the original state space, a saddle point in the corresponding Poincaré section) to the stable manifold of another saddle cycle or saddle point. The unstable manifold of the latter may then reconnect back to the original saddle cycle. The net effect of this heteroclinic cycle on a cluster of initial condition points is the same topologically as the effect of a homoclinic connection.

The effect of a homoclinic or heteroclinic tangle on a cluster of initial condition points can be seen elegantly in fluid mixing experiments. A two-dimensional fluid flow subject to a periodic perturbation may show chaotic trajectories for tracer particles suspended in the fluid. (We will explore this connection in more detail in Chapter 11.) Tracer particles injected near a saddle point (called a ***hyperbolic point*** in the fluid dynamics literature) show horseshoe type behavior with stretching, folding, and reinjection near the saddle point (see [Ottino, 1989] and OTT89 for beautiful pictures of these effects).

Local Lyapunov Exponent in a simulation of the Gulf of Mexico

https://www.youtube.com/watch?v=ljPhjmdxQGg

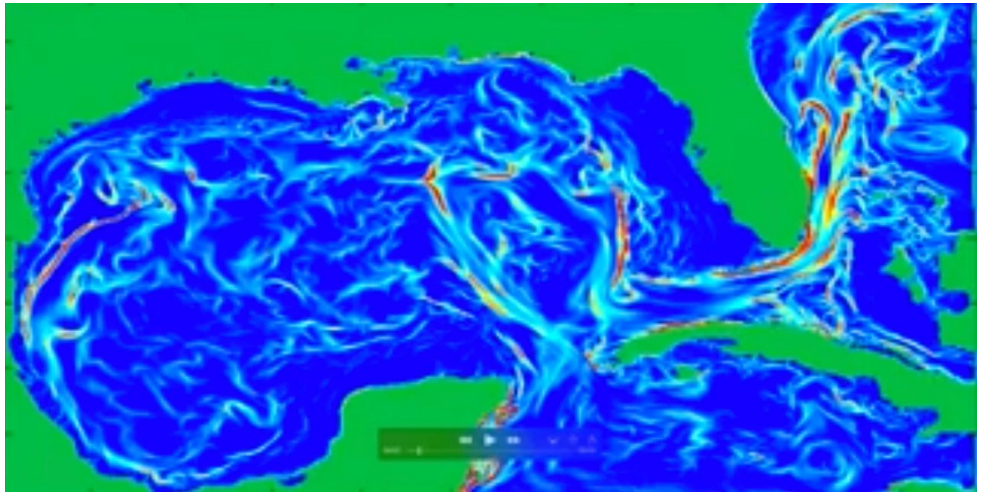

1.6 Determinism, Unpredictability, and Divergence of Trajectories

What is the importance of the divergence of nearby trajectories? We have claimed that this property is a signature of the kind of behavior we want to call chaotic and that this property allows us to distinguish between aperiodic behavior due to chaos and that due to external noise. The theoretical details will be taken up in later chapters. Here we want to discuss this behavior qualitatively.

The importance of divergence of nearby trajectories is the following: If a system, like the Lorenz model, displays divergence of nearby trajectories for some range of its parameter values, then the behavior of that system becomes essentially *unpredictable*. The system is still deterministic in the sense that if we knew the initial conditions of a trajectory exactly, then we could predict the future behavior of that trajectory by integrating the time-evolution equations for the system. If we make the smallest change in those initial conditions, however, the trajectory quickly follows a completely different path. Since there is always some imprecision in specifying initial conditions in any real experiment or real numerical calculation, we see that the actual future behavior is in fact unpredictable for a chaotic system. To make this point more forcefully, we like to say that the future of a chaotic system is *indeterminable* even though the system is *deterministic*.

CAOS DETERMINISTICO

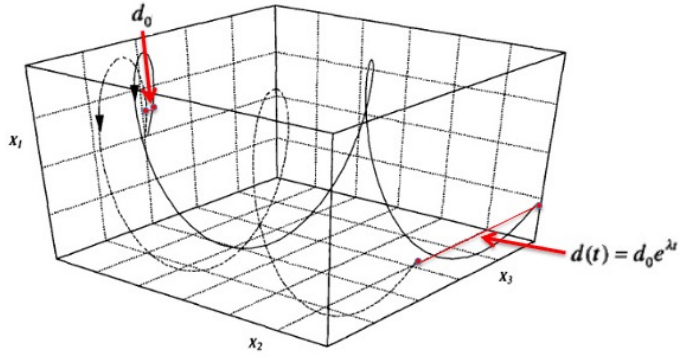

Fig. 4.1. A sketch of trajectories in a three-dimensional state space. Notice how two nearby trajectories can continue to behave quite differently from each other yet remain bounded by weaving in and out and over and under each other.

CAOS DETERMINISTICO

This unpredictability is related to the fact that we cannot write down a closed-form solution for the nonlinear equations used to describe the system. A closed-form solution is a "formula" $X(t) = X_o \tanh \pi (a\ t^2)$, for example, or a series solution, perhaps with an infinite number of terms, $X(t) = a_1(t) + a_2(t) + a_3(t)\ldots$. If such a closed-form solution could be found, then we could predict the future behavior of the system simply by evaluating the formula for some value of t corresponding to a future time. For a slightly different set of initial conditions, we would just evaluate the formula for those new initial conditions. Since the formula is presumably continuous in its dependence on parameters and initial conditions, small changes in those parameters and initial conditions would lead to small changes in $X(t)$. So, the large changes in $X(t)$ that occur for a chaotic system when we make small changes in the initial conditions cannot be represented by a closed-form solution. For a chaotic system, we must integrate the equations step-by-step to find the future behavior. (In essence we have to let the "experiment" run to find out what will happen.) The divergence of nearby trajectories means that any small error in specifying the initial conditions will be "magnified" as we integrate the equations. Thus, a small change in initial conditions leads to grossly different long-term behavior of the system, and we cannot in practice predict that long-term behavior in detail.

The unpredictability problem in nonlinear systems can be even worse than we imagine. For example, we might think that even though we cannot predict the detailed behavior of a trajectory, at least we know that the trajectory will end up within a particular attracting region in state space and will remain within that region. Unfortunately, many nonlinear systems have multiple attractors for a given set of parameter values. Trajectories starting at different state space points will end up on different attractors. Each attractor has its own basin of attraction. In some cases these basins have relatively simple geometric structures, and we can easily determine which initial conditions will lead to motion on the different attractors. In other cases, the basins can be so intertwined (forming so-called *riddled basins*) that even the smallest change in initial conditions can lead to a trajectory that ends up on a different attractor. In that case we lose even the modest ability to predict which attractor the trajectory will end up on (SOO93a) (LAW94)(LAI99).

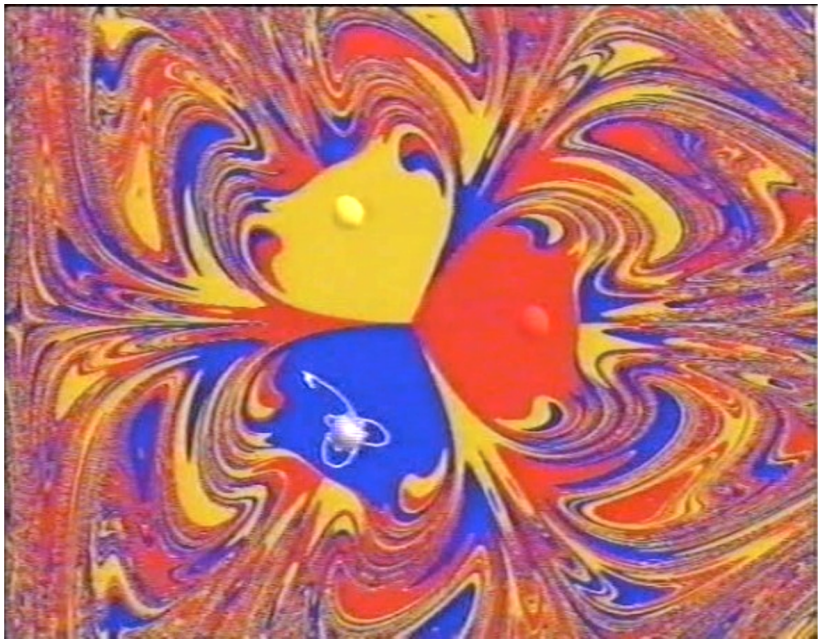

Dimensione frattale dell'attrattore caotico di Lorenz: D=2.06 ± 0.01

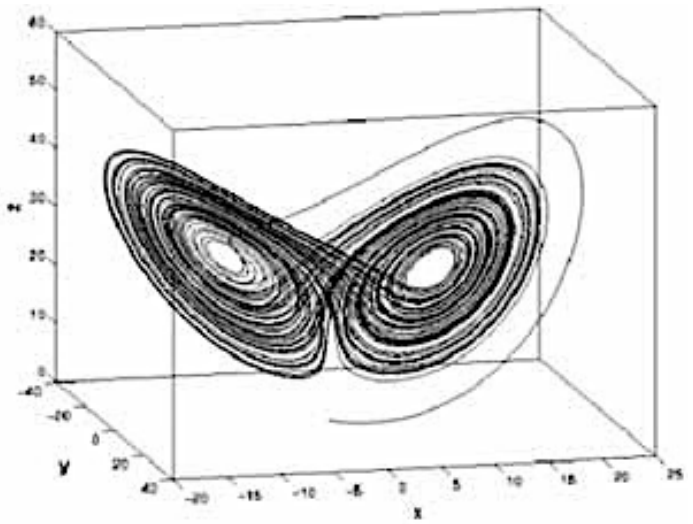

The effect of the divergence of nearby trajectories on the behavior of nonlinear systems has been expressed in an elegant metaphor known as the ***butterfly effect***. This metaphor first appeared in the title of a talk given by E. N. Lorenz[1] at the December 1972 meeting of the American Association for the Advancement of Science in Washington, D.C.: "Predictability: Does the Flap of a Butterfly's Wings in Brazil set off a Tornado in Texas." Earlier, Lorenz had used a seagull for this metaphor, but the name took an interesting Nabokovian twist with this paper's title. Lorenz's point was that if the atmosphere displays chaotic behavior with divergence of nearby trajectories or sensitive dependence on initial conditions, then even a small effect, such as the flapping of a butterfly's (or other avian creature's) wings would render our long-term predictions of the atmosphere (that is, the weather) completely useless.

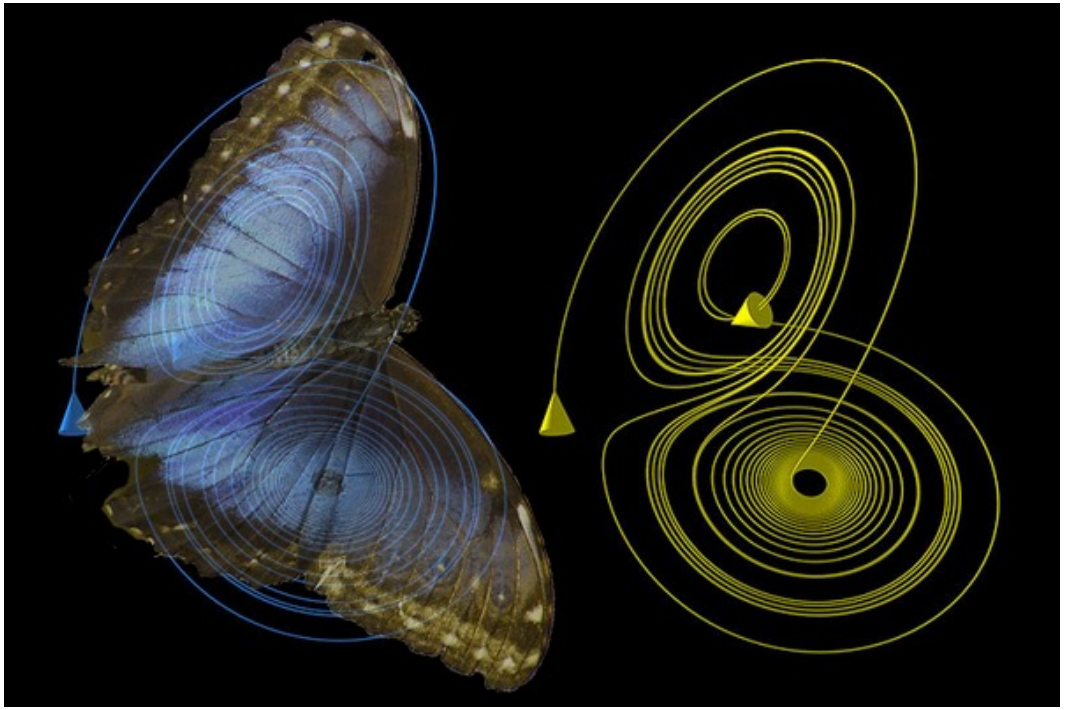

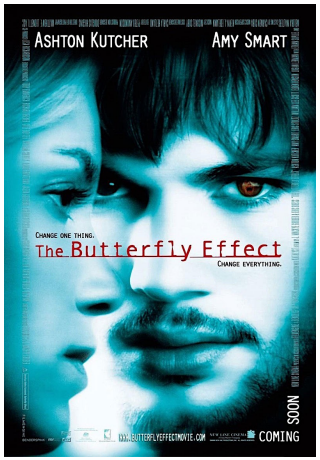

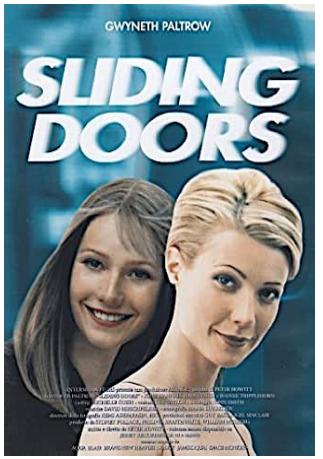

L’attrattore di Lorenz e l’effetto farfalla

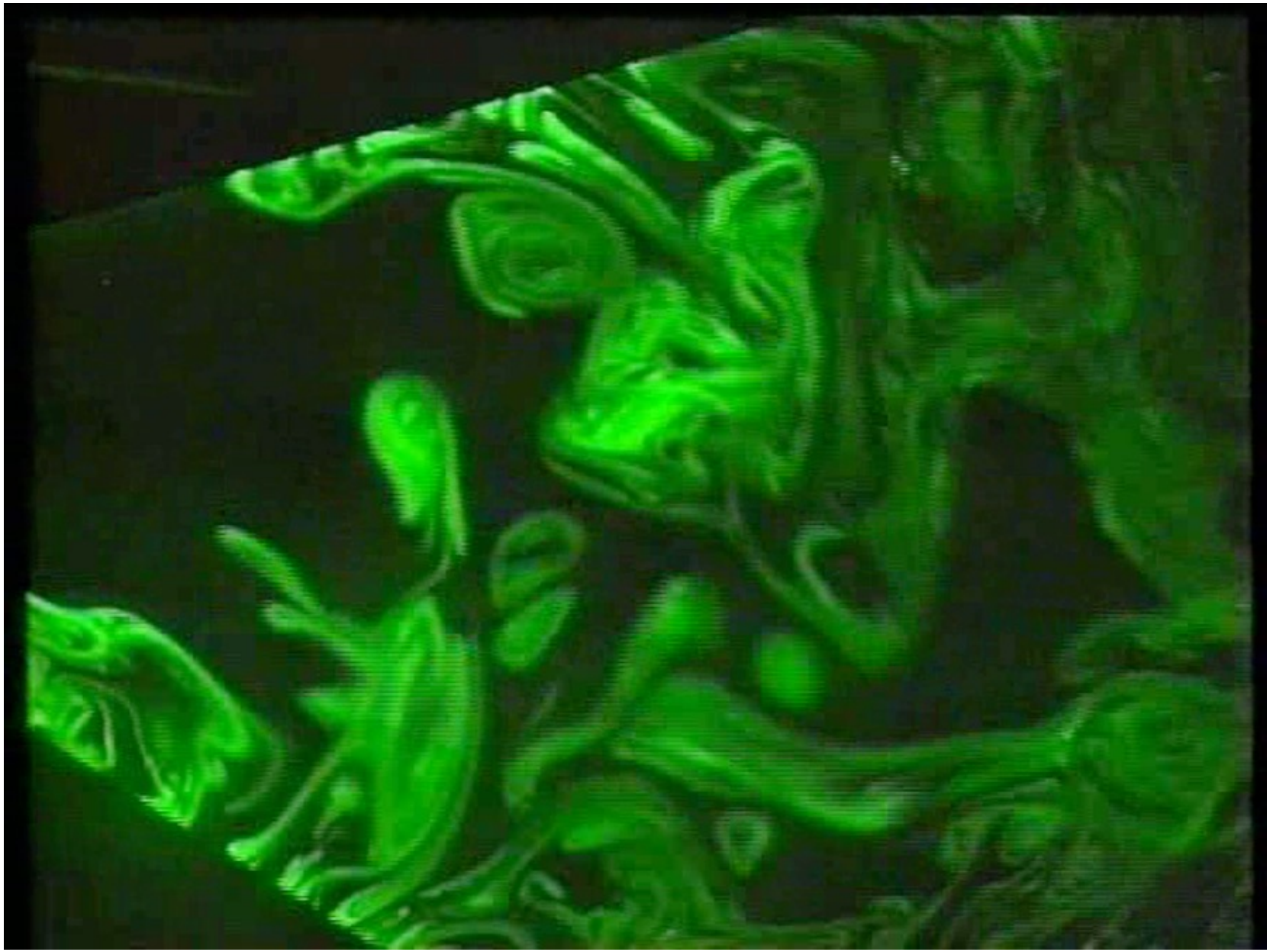

4.13 Lyapunov Exponents and Chaos

Our discussion of chaotic behavior has so far been qualitative. Now we want to introduce one method of quantifying chaotic behavior. There are two motivations here. First, we want some quantitative test for chaotic behavior; something that can, at least in principle, distinguish chaotic behavior from noisy behavior due to random, external influences. Second, we would like to have some quantitative measure of the degree of chaoticity; so, we can see how chaotic behavior changes as the system's parameters are changed. In this section, we will introduce Lyapunov exponents as one possible quantitative measure of chaos. In Chapter 5, we will describe how to find Lyapunov exponents for iterated maps. In Chapters 9 and 10, we will describe how to find Lyapunov exponents, as well as other quantifiers of chaos, from experimental data. In this section we will focus attention on dynamical systems described by a set of ordinary differential equations.

As we have seen in Section 3.7, a Lyapunov exponent is a measure of the rate of attraction to or repulsion from a fixed point in state space. In Section 4.2, we indicated that we could also apply this notion to the divergence of nearby trajectories in general at any point in state space. For a one-dimensional state space, let x_0 be one initial point and x a nearby initial point. Let $x_0(t)$ be the trajectory that arises from that initial point, while $x(t)$ is the trajectory arising from the other initial point. Then, if we follow the line of reasoning leading to Eq. (3.7-3), we can show that the "distance" s between the two trajectories, $s = x(t) - x_0(t)$ grows or contracts exponentially in time. Let us work through the details.

The time development equation is assumed to be

$$\dot{x}(t) = f(x) \tag{4.13-1}$$

Since we assume that x is close to x_0, we can use a Taylor series expansion to write

$$f(x) = f(x_0) + \left.\frac{df(x)}{dx}\right|_{x_0} (x - x_0) + \ldots \tag{4.13-2}$$

We now find that the rate of change of distance between the two trajectories is given by

$$\begin{aligned} \dot{s} &= \dot{x} - \dot{x}_0 \\ &= f(x) - f(x_0) \\ &= \left.\frac{df}{dx}\right|_{x_0} (x - x_0) \end{aligned} \tag{4.13-3}$$

where we have kept only the first derivative term in the Taylor series expansion of $f(x)$. Since we expect the distance to change exponentially in time, we introduce the Lyapunov exponent λ as the quantity that satisfies

$$s(t) = s(t=0)e^{\lambda t} \tag{4.13-4}$$

If we differentiate Eq. (4.13-4) with respect to time, we find

$$\begin{aligned} \dot{s} &= \lambda s(t=0)e^{\lambda t} \\ &= \lambda s \end{aligned} \tag{4.13-5}$$

Comparing Eq. (4.13-5) and Eq. (4.13-3) yields

$$\lambda = \left.\frac{df(x)}{dx}\right|_{x_0} \tag{4.13-6}$$

Thus we see that if λ is positive, then the two trajectories diverge; if λ is negative, the two trajectories converge.

In state spaces with two (or more) dimensions, we can associate a (local) Lyapunov exponent with the rate of expansion or contraction of trajectories for each of the directions in the state space. In particular, for three dimensions, we may define three Lyapunov exponents, which are the eigenvalues of the Jacobian matrix evaluated at the state space point in question. In the special case for which the Jacobian matrix has zeroes everywhere except for the principal (upper-left to lower-right) diagonal, the three eigenvalues (and hence the three local Lyapunov exponents) are given by

$$\lambda_1 = \frac{\partial f_1}{\partial x_1} \qquad \text{(4.13-7a)}$$

$$\lambda_2 = \frac{\partial f_2}{\partial x_2} \qquad \text{(4.13-7b)}$$

$$\lambda_3 = \frac{\partial f_3}{\partial x_3} \qquad \text{(4.13-7c)}$$

where the partial derivatives are evaluated at the state space point in question.

In practice, we know that the derivative of the time evolution function generally varies with x; therefore, we want to find an average of λ over the history of a trajectory. If we know the time evolution function, we simply evaluate the derivative of the time evolution function along the trajectory and find the average value. (For a dissipative, one-dimensional system, we know that this average Lyapunov exponent must be negative.)

We define a chaotic system to be a system which has at least one positive **average** Lyapunov exponent.

Behavior of a Cluster of Initial Conditions

To develop a geometric interpretation of the Lyapunov exponents, we consider a small rectangular volume of initial conditions with sides s_1, s_2, and s_3 surrounding this point with the sides oriented along the three state space axes. That volume will evolve in time as:

$$\frac{1}{V}\frac{dV}{dt} = \sum_{i=1}^{N}\frac{\partial f_i}{\partial x_i} \equiv div(f) \qquad V(t) = s_1 s_2 s_3 e^{(\lambda_1+\lambda_2+\lambda_3)t} \qquad (4.13\text{-}8)$$

If we compare Eq. (4.13-8) with Eq. (3.13-6), we see that the sum of the three Lyapunov exponents gives us the mathematical *divergence* of the set of time evolution functions. Again, in practice, we are interested in the average of these Lyapunov exponents over the history of a trajectory. For a dissipative system, the average of the sum of the exponents must be negative.

For a three-dimensional state space system described by a set of three first-order differential equations, one of the average Lyapunov exponents must be 0 unless the attractor is a fixed point (HAK83). (The 0 value for a Lyapunov exponent corresponds to the negligible attraction or repulsion of trajectories starting from nearby points that could be carried into each other by following the same trajectory for a short time.) Thus, for a dissipative system, at least one of the remaining average Lyapunov exponents must be negative. If the system is chaotic, one of the Lyapunov exponents is positive for a three-dimensional state space.

In state spaces with four (or more) dimensions, we might have more than one positive average Lyapunov exponent. In those cases, we say we have ***hyperchaos***. One possible route from periodic behavior to hyperchaotic behavior is discussed in HAL99.

It may be helpful to visualize what is happening with a more pictorial construction. For a dissipative system, we pick an initial point and let the resulting trajectory evolve until it is on the attracting region in state space. Then, we pick a trajectory point and construct a small sphere around it. Next, we follow the evolution of trajectories starting from initial points inside that sphere (some of which may not be on the attractor). In general, the sphere may be stretched in one direction and contracted in others as time goes on as shown schematically in Fig. 4.19. The sphere will be distorted into an ellipsoid. (For a dissipative system, the volume must contract to 0 if we follow the system long enough.)

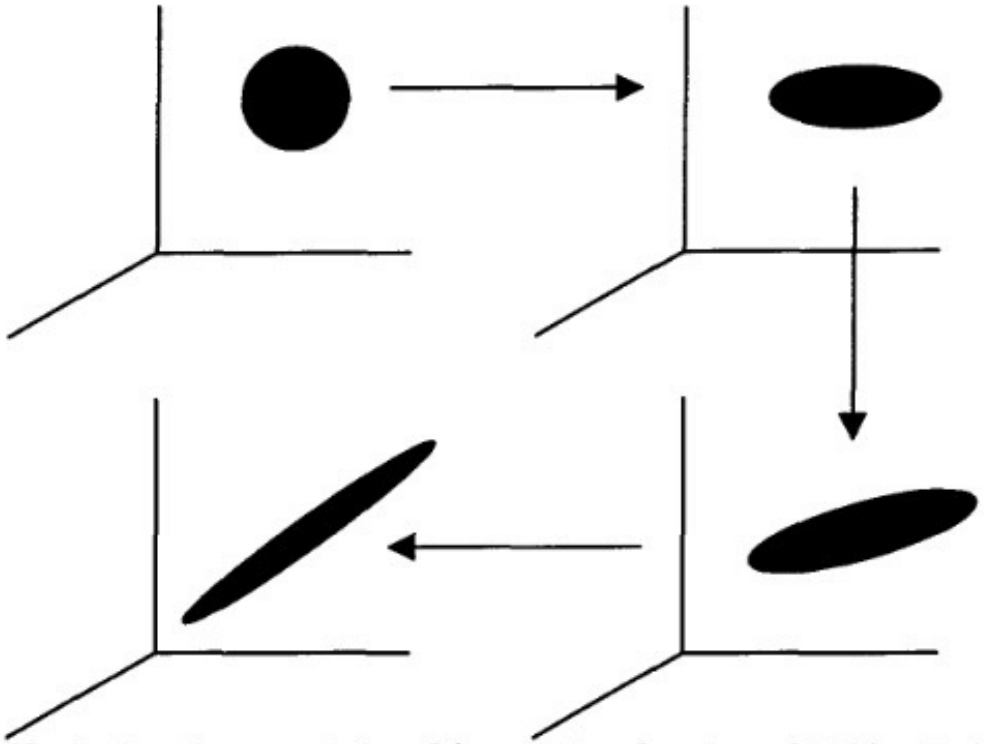

Fig. 4.19. A schematic representation of the evolution of a sphere of initial points in state space. The sphere starts in the upper-left-hand side. Time increases as we go clockwise around the figure. For a dissipative system, the volume associated with the set of initial points must go to 0. A chaotic system will exhibit exponential stretching of the sphere in at least one direction.

If we evaluate the (assumed) exponential rates of stretching and contraction for the different axes of the ellipsoid, we can find the Lyapunov exponents for that region of the attractor. Repeating this procedure along the trajectory allows us to calculate the set of average Lyapunov exponents for the system. This set of average Lyapunov exponents is called the ***spectrum of Lyapunov exponents***. If at least one of the average Lyapunov exponents is positive, then we conclude that the system displays (on the average) divergence of nearby trajectories and is "truly" chaotic. Table 4.3 summarizes the relationship between the spectrum of Lyapunov exponents and the type of attractor. (0, –, –) means that one of the Lyapunov exponents is zero and two are negative.

In practice the computation of these average Lyapunov exponents is complicated because the ellipsoid is rotated and distorted as the trajectories evolve. Various algorithms have been developed to calculate the Lyapunov exponents if the time evolution equations are known. The reader should consult the references given at the end of the chapter.

Table 4.3

Spectra of Lyapunov Exponents and Associated Attractors
Three–dimensional State Space

Signs of λs	Type of Attractor
(–,–,–)	Fixed Point
(0,–,–)	Limit Cycle
(0,0,–)	Quasi-Periodic Torus
(+,0,–)	Chaotic

If we evaluate the (assumed) exponential rates of stretching and contraction for the different axes of the ellipsoid, we can find the Lyapunov exponents for that region of the attractor. Repeating this procedure along the trajectory allows us to calculate the set of average Lyapunov exponents for the system. This set of average Lyapunov exponents is called the ***spectrum of Lyapunov exponents***. If at least one of the average Lyapunov exponents is positive, then we conclude that the system displays (on the average) divergence of nearby trajectories and is "truly" chaotic. Table 4.3 summarizes the relationship between the spectrum of Lyapunov exponents and the type of attractor. (0, –, –) means that one of the Lyapunov exponents is zero and two are negative.

In practice the computation of these average Lyapunov exponents is complicated because the ellipsoid is rotated and distorted as the trajectories evolve. Various algorithms have been developed to calculate the Lyapunov exponents if the time evolution equations are known. The reader should consult the references given at the end of the chapter.

Table 4.3

Spectra of Lyapunov Exponents and Associated Attractors
Three–dimensional State Space

Signs of λs	Type of Attractor
(–,–,–)	Fixed Point
(0,–,–)	Limit Cycle
(0,0,–)	Quasi-Periodic Torus
(+,0,–)	Chaotic